The Islamic University–Gaza
Research and Postgraduate Affairs
Faculty of Science
Master of Physics

الجامعـــــــة الإســـلاميـة– غـزة
شئون البحث العلمي والدراسات العليا
كليـــــــــــة العلـــــــــــوم
مـــاجـستيـــر الفيـــــزيـــاء

Characteristics of propagation of electromagnetic waves in slab waveguide structures comprising chiral and left-handed materials

خصائص انتشار الموجات الكهرومغناطيسية في موجهات موجات خطية تحتوي مواد كايرال ومواد يسارية

AlaaNaji Abu Helal

Supervised by

Dr.Sofyan A. Taya
Associate Professor of Physics

Dr.Khitam Y. Elwasife
Associate Professor of Physics

A thesis submitted in partial fulfillment of the requirements for the degree of Master of Science in Physics

Augest/2016

بسم الله الرحمن الرحيم

الجامعة الإسلامية-غزة
The Islamic University of Gaza
مكتب نائب الرئيس للبحث العلمي والدراسات العليا هاتف داخلي 1150

الرقم: Ref: ج س غ/35/
التاريخ: Date: 17/10/2016

نتيجة الحكم على أطروحة ماجستير

بناءً على موافقة شئون البحث العلمي والدراسات العليا بالجامعة الإسلامية بغزة على تشكيل لجنة الحكم على أطروحة الباحثة/ آلاء ناجي عبد الهادي أبوهلال لنيل درجة الماجستير في كلية العلوم قسم الفيزياء وموضوعها:

خصائص انتشار الموجات الكهرومغناطيسية في الموجهات الموجية المحتوية على مواد كايرل ومواد يسارية

Characteristics of propagation of electromagnetic waves in slab waveguide structures comprising chiral and left-handed materials

وبعد المناقشة العلنية التي تمت اليوم الاثنين 16 محرم 1438هـ، الموافق 2016/10/17م الساعة الواحدة ظهراً بمبني اللحيدان، اجتمعت لجنة الحكم على الأطروحة والمكونة من:

د. سفيان عبد الرحمن تايه	مشرفاً و رئيساً	.....
د. ختام يوسف الوصيفي	مشرفا	.....
د. معين فتحي عبيد	مناقشاً داخلياً	.....
د. هناء محمد موسى	مناقشاً خارجياً	.....

وبعد المداولة أوصت اللجنة بمنح الباحثة درجة الماجستير في كلية العلوم/ قسم الفيزياء.

واللجنة إذ تمنحها هذه الدرجة فإنها توصيها بتقوى الله ولزوم طاعته وأن تسخر علمها في خدمة دينها ووطنها.

والله ولي التوفيق،،،

نائب الرئيس لشئون البحث العلمي والدراسات العليا

أ.د. عبدالرؤوف علي المناعمة

إقـــــرار

أنا الموقع أدناه مقدم الرسالة التي تحمل العنوان:

Characteristics of propagation of electromagnetic waves in slab waveguide structures comprising chiral and left-handed materials

خصائص انتشار الموجات الكهرومغناطيسية في موجهات موجات خطية تحتوي مواد كايرال ومواد يسارية

أقر بأن ما اشتملت عليه هذه الرسالة إنما هو نتاج جهدي الخاص، باستثناء ما تمت الإشارة إليه حيثما ورد، وأن هذه الرسالة ككل أو أي جزء منها لم يقدم من قبل الاخرين لنيل درجة أو لقب علمي أو بحثي لدى أي مؤسسة تعليمية أو بحثية أخرى.

Declaration

I understand the nature of plagiarism, and I am aware of the University's policy on this.

The work provided in this thesis, unless otherwise referenced, is the researcher's own work, and has not been submitted by others elsewhere for any other degree or qualification.

Student's name: آلاء ناجي عبد الهادي أبو هلال اسم الطالب:

Signature: التوقيع:

Date: التاريخ:

Abstract

Characteristics of guided modes in slab waveguide structures which consist of chiral materials and left handed materials (LHMs) are analytically presented. We concentrate our study on chiral nihility materials, in which the permittivity and permeability are simultaneously zero.Two waveguide structures are studied in details.The first one is a symmetricslab waveguides in which the core consists of chiral nihility and the claddingsare left-handed meta-materialswhereas the second one is a symmetric slab waveguide in which the claddings are chiral nihility materials and the core layer is negative index materials**.**

The dispersion equation of an asymmetric three-layered slab waveguide in which all layers are chiral materialsis presented. Then, the dispersion equation of a symmetric one is derived. Forodd and even guided modes, the dispersion equations, normalized cutoff frequencies, electromagnetic fields and energy flow of right-handed and left-handed circularly polarized (RCP and LCP) modes are derived and plotted. Numerical results of guided low-order modes areprovided. Some novel features such as abnormal dispersion curves in the chiral nihility waveguides are found.

الملخص

هدف الدراسة هو دراسة خصائص انتشار الموجات الكهرومغناطيسية في موجهات موجات خطية تحتوي علي مواد كايرال ومواد يسارية بطريقة تحليلية. تم تركيز الدراسة علي مواد كايرال يكون فيها النفاذية الكهربائية والنفاذية المغناطيسية تؤول الي الصفر. تم اعتماد هيكلين لموجهات الموجات قيد الدراسة اولهما هيكل يحتوي في الطبقة الاساسية مواد كايرال ذات نفاذية كهربائية ومغناطيسية صفرية والطبقة المحيطة (الغلاف) يحتوي علي مواد يسارية اما الاخر فيتكون من مواد يسارية في الطبقة الاساسية ومواد كايرال بمعاملات نفاذية كهربائية ومغناطيسية صفرية في الطبقة المحيطة (الغلاف).

تم اشتقاق معادلات التشتت اولا لهيكل موجه موجي غير متماثل يحتوي في طبقاته الثلاثة مواد كايرال ثم اشتقاق معادلات التشتت للهيكلين سابقي الذكر. ثم تناولت الدراسة تفصيل خصائص انتشار الموجات في الانماط الزوجية والفردية للهيكلين والانماط يمينية ويسارية الاستقطاب. من خلال الرسم تم اكتشاف خصائص مميزة وفريدة لمنحني انتشار الموجات.

Dedication

This thesis work is dedicated to my husband, Tawfeek, who has been a constant source of support and encouragement during the challenges of graduate and life. I am truly thankful for having you in my life.

This work is also dedicated to my parents, Naji and Samia Abu Helal, who have always loved me unconditionally and whose good examples have taught me to work hard for the things that I aspire to achieve.

I will not forget my daughters, Shaimaa and Sham, for their patience.

Acknowledgment

First and above all, I praise God, the almighty for providing me this opportunity and granting me the capability to proceed successfully.This thesis owes its existence to the help, support and inspiration of severalpeople. Iwould first like to thank my thesis advisor ***Dr. Sofyan A. Taya*** of the Faculty of Science, Physics Department, at The Islamic University of Gaza. The door to Dr. Tayaoffice was always open whenever I ran into a trouble spot or had a question about my research or writing. He consistently allowed this paper to be my own work, but steered me in the right direction whenever he thought I needed it.

I am alsolike to express my sincere appreciation and gratitude to ***Dr. Khitam Y. Elwasife*** of the Faculty of Science, Physics Department, at The Islamic University of Gaza, for her guidance during my research.Her support and inspiringsuggestionshave been precious for the development of this thesis content.

I am also indebted to***Dr. Tahany R. Dalloul*** and ***Ms.HanaaElejla***, whome have been a constant source of encouragement and enthusiasm, not only during this thesis projectbut also during the two years of my Master program.

I would never forget all the chats and beautiful moments I shared with some of my friends and classmates. They were fundamental in supporting me during these stressful and difficult moments.

Also, I know that you did not want to be named, a person that believed in my power and supported me. My lovely husband, Dear ***TawfeekAljalees*** thanks you foryour immeasurable patience during the years of studies, projects, and telephone chats.

My deepest gratitude goes to ***my family, my parent, my sisters and brothers*** for their unflagging love and unconditional support throughout my life and my studies.You made me live the mostunique, magic and carefree childhood that has made me who I am now!

And finally, I warmly thank and appreciate ***my mother and father-in-law*** fortheirmaterialandspiritual support in all aspects of my life.

Table of Contents

List of Figures

Chapter 1

Introduction

Chapter1

Introduction to Electromagnetic and Waveguide Theories

1.1 Electromagnetic theory

James Clark Maxwell (1831-1879) unified the most important experimental laws on electromagnetic, which presented by previous scientists and formulated a symmetric coherent set of equations governing the behaviour of the macroscopic electromagnetic phenomenon. These equations are known as Maxwell's equations.

1.1.1 Maxwell's equations and constitutive relations

Maxwell's equations obtained theoretically the speed of an electromagnetic wave which matches the experimental value for the speed of light, within a small experimental error. In fact, the form that we know today was first expressed by Oliver Heaviside (1850-1925), but Maxwell was the first to show them clearly.
The basic Maxwell equations in derivative form are given by

$$\nabla \times \vec{E} = -\frac{\partial \vec{B}}{\partial t} \qquad \text{Faraday's Law} \qquad (1.1)$$

$$\nabla \times \vec{H} = \frac{\partial \vec{D}}{\partial t} + J \qquad \text{Ampere's Law} \qquad (1.2)$$

$$\nabla . \vec{D} = \rho \qquad \text{Gaus's Law} \qquad (1.3)$$

$$\nabla . \vec{B} = 0 \qquad \text{No magnetic monopoles} \qquad (1.4)$$

These equations are reasonable for any medium as well as vacuum. Where $\vec{E}$ in volts per meter (V/m) is the electric field, ρ in coulombs per cubic meter (C/m^3) is the electric charge density, J in amperes per square meter (A/m^2) is the electric current density, $\vec{D}$ in coloumbs per square meter (C/m^2) is the electric induction vector, known as the electric displacement vector or electric flux density and $\vec{H}$ in amperes

per meter (A/m), is the magnetic strength vector, $\vec{D}$ and $\vec{H}$ are related to $\vec{E}$ and $\vec{B}$ through

$$\vec{\mathrm{D}} = \varepsilon_0 \vec{\mathrm{E}} + \vec{\mathrm{P}} \tag{1.5}$$

$$\vec{\mathrm{H}} = \vec{\mathrm{B}}/\mu_0 - \vec{\mathrm{M}}, \text{ or } \vec{\mathrm{B}} = \mu_0 (\vec{\mathrm{H}} + \vec{\mathrm{M}}) \tag{1.6}$$

where the polarization vector $\vec{P}$ is the volume density of electric dipole moment and the magnetization vector $\vec{M}$ is the volume density of magnetic dipole moment. ε_0 and μ_0 are two constants corresponds to the permittivity and the permeability of vacuum, respectively. They are given the values of $\mu_0 = 4\pi \times 10^{-7}$ H/m and $\varepsilon_0 = 8.85418782 \times 10^{-12}$ F/m.The relation between $\vec{P}$ and $\vec{E}$, or the relation between $\vec{M}$ and $\vec{H}$, is usually called the constitutive relations. In vacuum, we have $\vec{P} = 0$ and $\vec{M} = 0$, or $\vec{\mathrm{D}} = \varepsilon_0 \vec{\mathrm{E}}$ and $\vec{\mathrm{B}} = \mu_0 \vec{\mathrm{H}}$.Different kinds of media introduce different constitutive relations, such that

● Simple media which is non-dispersive, linear and isotropic, these relationships can be written as

$$\begin{aligned} \vec{P} &= \varepsilon_0 \chi_e \vec{E} \\ \vec{M} &= \chi_m \vec{H} \end{aligned} \tag{1.7}$$

where χ_e and χ_m is the electric susceptibilityand the magnetic susceptibility of the medium, respectively. Thus the constitutive relations of the simple media reads

$$\vec{D} = \varepsilon_0 \left(1 + \chi_e\right) \vec{E} = \varepsilon_0 \varepsilon_r \vec{E}; \quad \text{or } \vec{D} = \varepsilon \vec{E} \tag{1.8}$$

$$\vec{B} = \mu_0 \left(1 + \chi_m\right) \vec{H} = \mu_0 \mu_r \vec{H}; \quad \text{or } \vec{B} = \mu \vec{H} \tag{1.9}$$

in which $\varepsilon = \varepsilon_0 \varepsilon_r$ and $\mu = \mu_0 \mu_r$, where ε and μ are permittivity and permeabilityof the medium, respectively.ε_r and μ_r are relative permittivity and relative permeability, respectively.

● Dispersive media where $\vec{D}$ depends on the time derivatives of all orders of $\vec{E}$. Also $\vec{B}$ and $\vec{H}$ have the same behavior. The constitutive relations become linear differential equations in the form

$$\vec{D} = \varepsilon \vec{E} + \varepsilon_1 \frac{\partial \vec{E}}{\partial t} + \varepsilon_2 \frac{\partial^2 \vec{E}}{\partial t^2} + \ldots \tag{1.10}$$

$$\vec{B} = \mu \vec{H} + \mu_1 \frac{\partial \vec{H}}{\partial t} + \mu_2 \frac{\partial^2 \vec{H}}{\partial t^2} + \ldots \tag{1.11}$$

● Nonlinear media in which the parameters ε and μ depend on the field strengths. Also, they are functions of $\vec{E}$ and $\vec{B}$.

● Anisotropic media where polarization depends on $\vec{E}$ location and time. So does $\vec{M}$.

$$\vec{\mathrm{D}} = \varepsilon \vec{\mathrm{E}} \ , \ \vec{\mathrm{B}} = \mu \vec{\mathrm{H}} . \tag{1.12}$$

where ε is the tensor permittivityand μ is the tensor permeability, taking the form

$$\varepsilon = \begin{bmatrix} \varepsilon_{xx} & \varepsilon_{xy} & \varepsilon_{xz} \\ \varepsilon_{\mathrm{yx}} & \varepsilon_{yy} & \varepsilon_{yz} \\ \varepsilon_{zx} & \varepsilon_{zy} & \varepsilon_{zz} \end{bmatrix} \quad , \quad \mu = \begin{bmatrix} \mu_{xx} & \mu_{xy} & \mu_{xz} \\ \mu_{\mathrm{yx}} & \mu_{yy} & \mu_{yz} \\ \mu_{zx} & \mu_{zy} & \mu_{zz} \end{bmatrix}$$

● Bi-isotropic and bi-anisotropic media where cross coupling between the electric and magnetic fields take place. These media become polarized and magnetized at the

same time when placed in an electric or magnetic field. The general constitutive relations are given by

$$\vec{D} = \varepsilon . \vec{E} + \xi . \vec{H} \tag{1.13}$$

$$\vec{B} = \zeta . \vec{E} + \mu . \vec{H} \tag{1.14}$$

where ε, ζ, ξ, and μ are generally some of them are 3x3 tensors and some are scalars (Zhang and Li, 2008; Griffiths,1999).These media will be introduced in details in the next chapter.

1.1.2 Boundary conditions

The solution of electromagnetic problems becomes much easier if we study the behavior of electromagnetic fields on the boundary or the interface between two media. The boundary conditionscan be summarized as (Zhang and Li, 2008; Griffiths, 1999).

1. The normal component of the magnetic flux is continuous across the surface of discontinuity i.e.

$$\vec{n} . (\vec{B}_2 - \vec{B}_1) = 0 \tag{1.15}$$

2. The normal component of the electric displacement is discontinuous by ρ, if a surface charge of density ρexists, then

$$\vec{n} . (\vec{D}_2 - \vec{D}_1) = \rho \tag{1.16}$$

3. The tangential component of the electric field is continuous across the surface, i.e.

$$\vec{n} \times (\vec{E}_2 - \vec{E}_1) = 0 \tag{1.17}$$

4. The tangential component of the magnetic field is discontinuous across the surface by J, if a surface current of density J exists, then

$$\vec{n} \times (\vec{H}_2 - \vec{H}_1) = J \tag{1.18}$$

1.1.3 Wave equations

The wave equationscan be derived directly from Maxwell's equations. It gives the space and time dependence of the electric and magnetic field vector. The wave equations are partial differential equations of second order (Thide, 2004). In the source-free region, where $\rho = 0$ and $J = 0$, we want to derive the wave equation for the $\vec{E}$ and $\vec{B}$ fields. Maxwell's equations,using the constitutive relations (1.8) and (1.9), now take the form

$$\nabla \times \vec{E} = -\frac{\partial \vec{B}}{\partial t} \tag{1.19}$$

$$\nabla \times \vec{B} = \epsilon\mu \frac{\partial \vec{E}}{\partial t} \tag{1.20}$$

$$\nabla . \vec{E} = 0 \tag{1.21}$$

$$\nabla . \vec{B} = 0 \tag{1.22}$$

Taking the curl of Eq. (1.19), we have

$$\nabla \times \nabla \times \vec{E} = -\epsilon\mu \frac{\partial^2 \vec{E}}{\partial t^2} \tag{1.23}$$

Using the vector identity, the handy "BAC-CAB" formula

$$\vec{A} \times \left(\vec{B} \times \vec{C} \right) = \vec{B} \left(\vec{A} . \vec{C} \right) - \vec{C} \left(\vec{A} . \vec{B} \right) \tag{1.24}$$

The wave equation have the form (Zhang and Li, 2008; Griffiths, 1999)

$$\nabla^2 \vec{E} - \epsilon\mu \frac{\partial^2 \vec{E}}{\partial t^2} = 0, \tag{1.25}$$

For steady-state sinusoidal time-dependent fields, we assume an electromagnetic wave propagates at a single angular frequency ω (in radians per meter). A vector that represents the electromagnetic field is, in the phasor notation, i.e.

$$\vec{\psi}(r,t) = \psi_0(r)\, e^{j\omega t}, \tag{1.26}$$

where $\vec{\psi}$ is either $\vec{E}$ or $\vec{H}$, ψ_0 is the amplitude of the wave (Zhang and Li, 2008; Griffiths, 1999). Using the following substitutions in Maxwell Eq.(1.19) and Eq.(1.20) we get

$$\frac{\partial}{\partial t} \to j\omega, \qquad \frac{\partial^2}{\partial t^2} \to -\omega^2 \tag{1.27}$$

We have

$$\vec{\nabla} \times \vec{E} = -j\omega \vec{B} = -j\omega\mu \vec{H}, \tag{1.28}$$

$$\vec{\nabla} \times \vec{H} = j\omega \vec{D} = j\omega\varepsilon \vec{E}, \tag{1.29}$$

The wave equation (1.25) of $\vec{E}$ becomes

$$\nabla^2 \vec{E} + k^2 \vec{E} = 0, \tag{1.30}$$

where $k^2 = \varepsilon\mu\omega^2$, is the wave number. The wave equation can be written for $\vec{H}$-field,

$$\nabla^2 \vec{H} + k^2 \vec{H} = 0 \tag{1.31}$$

Eqs. (1.25), (1.30) and (1.31)are three dimensional equations called Helmholtz equations (Thide,2004; Zhang and Li, 2008; Griffiths, 1999). where the laplacian operator ∇^2 is given in rectangular coordinates by

$$\nabla^2 = \frac{\partial^2}{\partial x^2} + \frac{\partial^2}{\partial y^2} + \frac{\partial^2}{\partial z^2}, \tag{1.32}$$

1.1.4 Wave parameters

By deriving the wave equations we end up with a wave velocity (Thide, 2004) equal to

$$v = \frac{1}{\sqrt{\varepsilon\mu}}, \tag{1.33}$$

The index of refraction or the refractive index, n, is defined by (Griffiths, 1999).

$$n = \frac{c}{v} = \sqrt{\frac{\varepsilon\mu}{\varepsilon_0\mu_0}}, \tag{1.34}$$

where, c is the speed of light in vacuum given the value, $c = \frac{1}{\sqrt{\varepsilon_0\mu_0}} = 3*10^8 \frac{\text{m}}{\text{s}}$.

The electromagnetic wave which represents the solution of the wave equation takes the form

$$\vec{\psi}(r,t) = \psi_0 e^{-j(\vec{k}.\vec{r}-\omega t)}, \tag{1.35}$$

Since $\vec{k}$ is the wave vector . It likes any vector has a magnitude and direction. Its magnitude is the wave number (k), which is inversely proportional to the wavelength and its direction is ordinarily the direction of wave propagation(Thide, 2004), i.e.

$$k = \frac{\omega}{c} n = \frac{2\pi}{\lambda} n \tag{1.36}$$

In vacuum, the wave number is $k_0 = 2\pi / \lambda_0$. Consequently, we can obtain the wave number in a medium if the refractive index is known

$$k = n k_0 \tag{1.37}$$

1.1.5 Poyntingvectors

The product of electric and magnetic fields is related to the energy of the electromagnetic wave (Zhang and Li, 2008) since the voltage is the integral of electric field and the magnetic field is created by current. Thus

$$\vec{S} = \vec{E} \times \vec{H} \tag{1.38}$$

is the energy that passes through a unit area per unit time. It is called a Poyntingvector. For an electromagnetic wave propagating at a single angular frequency ω, Poynting vector $\vec{S}$ is given as

$$\vec{S} = \frac{1}{2}\mathrm{Re}(\vec{E} \times \vec{H}^{*}) \tag{1.39}$$

where $\vec{H}^{*}$ is the complex conjugate of $\vec{H}$ (Griffiths, 1999).

1.1.6 Reflection and transmission of plane waves

When a monochromatic electromagnetic plane wave is incident at an oblique angle θ_i on a boundary between two linear, homogeneous and isotropic media with different refractive indices, a portion of this wave is reflected at angle θ_r, and another portion is transmitted at angle θ_t (Markoš and Soukoulis, 2008). The three angles are shown in Figure (1.1).

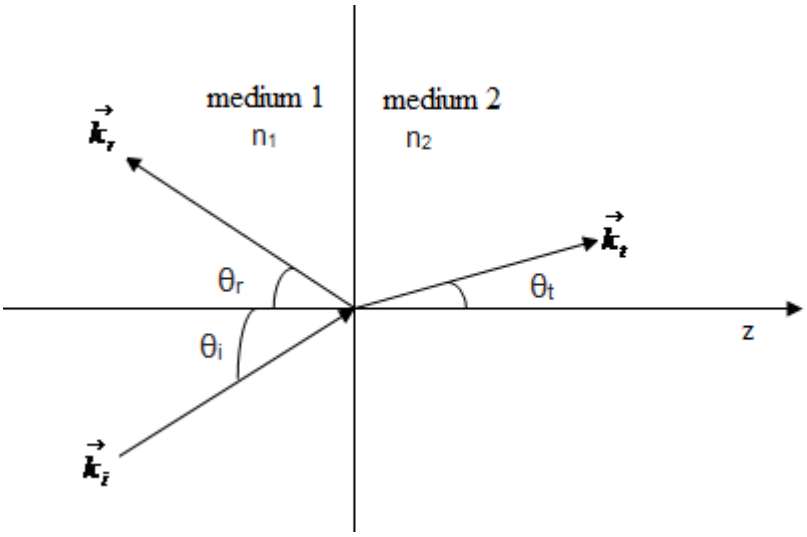

Figure (1.1): An electromagnetic wave incident at a plane interface.

The three laws of geometrical optics which govern this phenomenon are (Griffiths, 1999)

- All wave vectors $\vec{k}$ lie in a common plane: the three wave vectors $\vec{k}_i$, $\vec{k}_r$ and $\vec{k}_t$ all lie in a plane known as the plane of incidence includes the unit normal to the interface.
- Law of Reflection: the angle of incidence is equal to the angle of reflection i.e. $\theta_i = \theta_r$.
- Law of Refraction – Snell's Law: which states that $n_1 \sin\theta_i = n_2 \sin\theta_t$.

The reflectivity of light depends upon the angle of incidence and the plane of polarization of the light. There are three possible polarization cases to consider

Case (I): known as transverse electric (TE) polarization, occur when $\vec{E}_{inc}$ is perpendicular to the plane of incidence and $\vec{B}_{inc}$ is parallel to the plane of incidence.

Case (II): known as transverse magnetic (TM) polarization, occur when $\vec{E}_{inc}$ is parallel to the plane of incidence and $\vec{B}_{inc}$ is perpendicular to the plane of incidence.

Case (III): The most general case, is a linear vector combination of Cases (I) and (II) above, occur when $\vec{E}_{inc}$ is neither parallel nor perpendicular to the plane of incidence and $\vec{B}_{inc}$ is neither parallel nor perpendicular to the plane of incidence.

Although, Snell's Law can be used to relate the incident and transmitted angles, Fresnel's equations describe the reflection (r) and transmission (t) coefficients of electromagnetic waves at the boundary and can be stated in terms of the angles of incidence and transmission for nonmagnetic media as

$$r_{TE} = \frac{n_i \cos\theta_i - n_t \cos\theta_t}{n_i \cos\theta_i + n_t \cos\theta_t} \tag{1.40}$$

$$r_{TM} = \frac{n_t \cos\theta_i - n_i \cos\theta_t}{n_i \cos\theta_t + n_t \cos\theta_i} \tag{1.41}$$

$$t_{TE} = \frac{2n_i \cos\theta_i}{n_i \cos\theta_i + n_t \cos\theta_t} \tag{1.42}$$

$$t_{TM} = \frac{2n_i \cos\theta_i}{n_i \cos\theta_t + n_t \cos\theta_i} \tag{1.43}$$

For a special angle of incidence where the reflection coefficient, is equal to zero, i.e. no reflected wave exists. This angle is known as the Brewster angleand is denoted by θ_B. Generally, Brewster angle is given by

$$\tan\theta_B = \frac{n_2}{n_1} \tag{1.44}$$

At the boundary between nonmagnetic dielectrics, i.e. for an interface between two right-handed materials of positive refractive indices, the Brewster angle exists for only the (TM) wave, while the incident angle of zero reflection for the (TE) wave does not exist. Furthermore, we can see that the Brewster angle exists for only the

(TE) wave when we treat the formula for the reflection coefficient for the boundary between magnetic media. While if one of the media is a left handed material with negative index of refraction, Brewster angle can be found for both polarizations(Thide, 2004; Zhang and Li, 2008).

1.1.7 Total internal reflection

When an incident plane wave passes from an optically dense medium into an optically rarer medium, i.e. $n_1 > n_2$another special angle of incidence called a critical angle θ_c exists(Thide, 2004; Zhang and Li, 2008). Where no transmitted wave and the refracted wave is propagated parallel to the boundary $\theta_t = 90^\circ$. This angle does not depend on polarization, it is actually defined by Snell's law and given by

$$\sin\theta_c = \frac{n_2}{n_1} \tag{1.45}$$

If the angle of incidence exceeds the critical angle, $\theta_i > \theta_c$, the wave comes back into the same medium after reflection from interface. This total reflection phenomenon at the boundary of two nonconducting media is also known as total internal reflection.

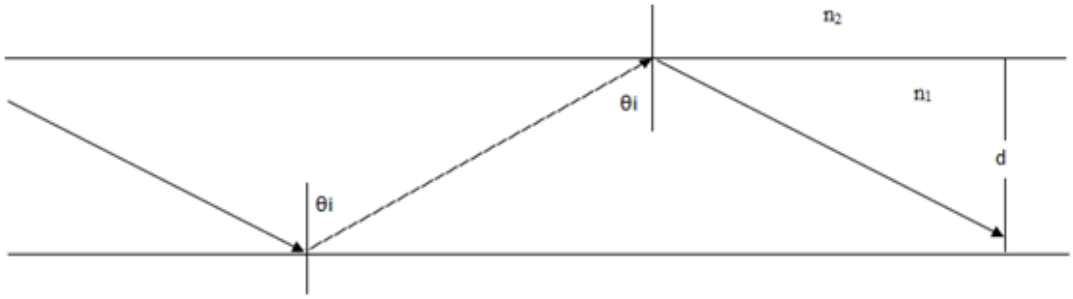

Figure (1.2): Total internal reflection of light beam(TIR).

1.2 Waveguides theory

Waveguides (Kapany andBurke, 1997) are the structures that are used to guide and confine electromagnetic waves.Waveguides are classified to as either metal waveguides or dielectric waveguides. Metal waveguides are assumed as one enclosed conductor filled with an insulating medium but the dielectric waveguides consists of multiple dielectrics and the electromagnetic wave propagates along the

waveguide by reflections at the boundaries. The optical fiber, usually has a circular cross-section, is a well known dielectric waveguide, even though the planar slab waveguide are the simplest dielectric guide which widely used in integrated optics. Also, there are many different structures of waveguides. Depending on the frequency of the wave to be transmitted, the amount of power to be transferred, and the amount of losses one can choose the suitable structure.These structures are

- Coaxial cables are widely used in radio frequencies (RF) below 3 GHz above that the losses are too enormous.
- Two-wire lines which can radiate at microwave frequencies .
- Micro strip lines are used widely in microwave integrated circuits.
- Rectangular waveguides are used at frequencies greater than 3GHz to transfer large amounts of microwave power.

1.2.1 Waveguide structure

The structure to be discussed is the planner slab waveguide with its simplest form shown in Figure (1.3). The figure shows a planner film having a refractive index n_f sandwiched between two materials called cover and substrate with lower refractive indices n_c and n_s respectively. The fields will either be symmetric or asymmetric, due to the symmetry of the geometry. In order to confine the field, the fields outside the slab must be evanescent, i.e. they decay in the x direction. Moreover, the plane wave inside bounces back and forth due to total internal reflection (Griffiths, 1999).

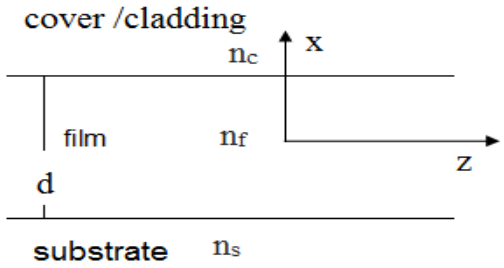

Figure (1.3): Planner waveguide structure.

The propagation of the field can be characterized as a sum of two plane TEM waves, upward and downward waves, propagating along zig-zag paths between the guide walls, with total internal reflection of the light at the film-substrate and film-cover

interfaces (Kapany and Burke, 1997). These waves are monochromatic and coherent travelling with a wave vector $\vec{k}$ and having an angular frequency ω. There are limited frequencies and forms for the wave function which can propagate in the waveguide due to the constraints of the boundary conditions. The lowest frequency for the mode to propagate is the cutoff frequency of that mode. The mode with the lowest cutoff frequency is the basic mode of the waveguide, and its cutoff frequency is the waveguide cutoff frequency. In order to design the suitable waveguide structure, the dispersion relation becomes so important. The dispersion equation of the guide yielding the propagation constant β as a function of the frequency ω and the film thickness d.It is often convenient to use the effective refractive index (N) of the guide, which is defined by

$$N = \frac{\beta}{k} \tag{1.46}$$

where $\vec{k}$ is the wave vector.The guide may be symmetric or asymmetric guide due to the matches between n_c and n_s.

1.2.2 Modes in waveguide

The modes of the guide are the solutions of the wave equations taking the standard form

$$\vec{E}(x, y, z) = \vec{E}(x, y) \exp(-j\beta z) \tag{1.47}$$

$$\vec{H}(x, y, z) = \vec{H}(x, y) \exp(-j\beta z) \tag{1.48}$$

According to which of the longitudinal components are zero, we may classify the solutions as

- Transverse electric and magnetic (TEM) mode, $E_z = 0$, $H_z = 0$.
- Transverse electric (TE) mode, $E_z = 0$, $H_z \neq 0$.
- Transverse magnetic (TM) mode, $E_z \neq 0$, $H_z = 0$.
- Hybrid mode, $E_z \neq 0$, $H_z \neq 0$ (Griffiths, 1999).

1.2.3 Goos-Hänchenshift

When the electromagnetic wave reaches the interface between the film and the cladding, it penetrates in the cladding until a specific depth before suffering reflection this cause the reflected wave is shifted relative to the incident wave. This ray shift, shown in Figure (1.4), is so called the Goos-Hänchen Shift (Markoš and Soukoulis, 2008).

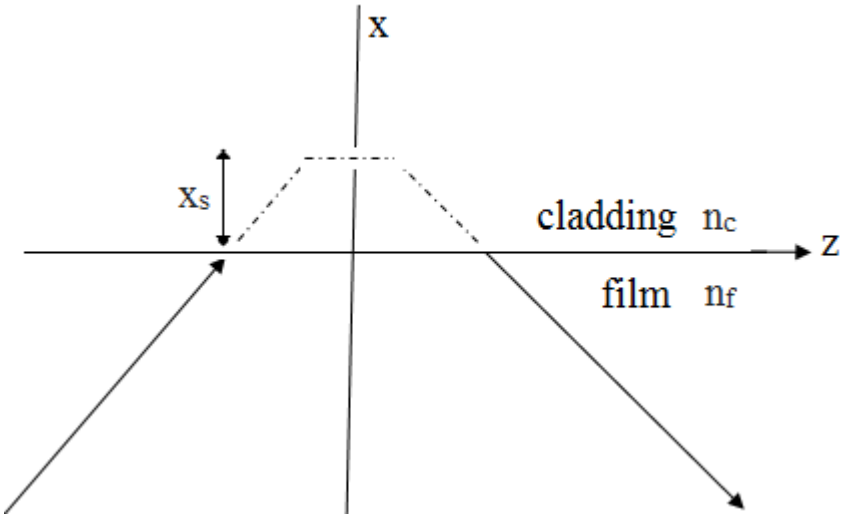

Figure (1.4): Ray picture showing the Goos-Hänchen shift.

Chapter 2
Left-Handed and Chiral Metamaterials

Chapter 2
Left-Handed and Chiral Metamaterials

2.1 History of left handed materials

Metamaterials are artificial media composed of elements which dimension are small compared to the wavelength of interest. Metamaterials may display properties which are more noticeable than those observed in natural materials. The famous example of these properties are metamaterials with a negative refractive index which are well known as negative index metamaterials (NIMs), also called left handed materials (LHMs). The general consideration of the electrodynamics properties of the materials with simultaneously negative values of the dielectric permittivity ε and magnetic permeability μ had been introduced by Veselago, in 1968 (Veselago, 1968). Veselago presented that when the algebraic sign of real parts of the permittivity and permeability are the same, electromagnetic waves will propagate. Otherwise, waves will not propagate in a medium. Also, he showed that LHMs have the ability to support backward waves. The concept to fabricate metamaterials with negative index of refraction seemed to be unfamiliar and new, so Veselago's work placed dormant for nearly 30 years. Pendryand co-workers (1996) released that the concept to make LHMs is to treat permitivity and permeability separately, so he used thin wire structure (wire array) to produce negative permitivity and magnet-free split-ring resonator (SRR) structure to produce negative permeability (Pendry, Holden, Robbins and Stewart, 1999). Recently though, much attention of this kind of metamaterials has been drawn and the fabrication of perfect lens where an object can be recreated without any error in diffraction was allowed (Pendry, 2000). LHMs has been first experimentally observed by Shelby, Smith, and Shultz (Shelby, Smith and Schultz, 2001) in completely different systems.

2.2 Electromagnetic properties and applications of left-handed materials

2.2.1 Reversal of Snell's law

It is noticeable from Eq. (1.38) that the Poynting vector $\vec{S}$ is given by a right-handed rule, as well as the wave vector $\vec{k}$. However, when the medium has a

negative value of permitivity and permeability these vectors become left handed and both of $\vec{S}$ and $\vec{k}$ propagate in opposite direction as explain in Figure (2.1) . Note that, the electromagnetic wave propagates in the direction of the Poynting vector $\vec{S}$ where the direction of the group velocity.

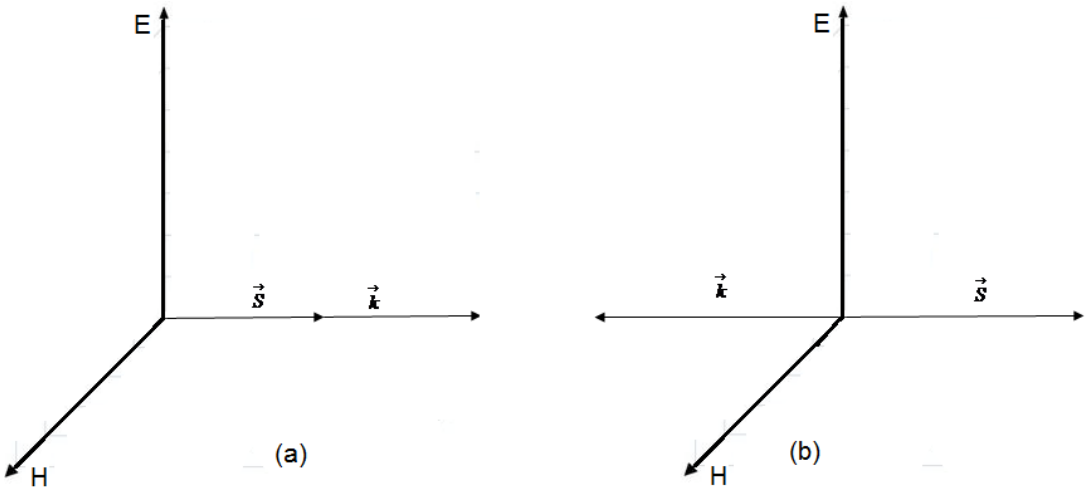

Figure(2.1): Propagation of the wave vector $\vec{k}$ and Poynting vector $\vec{S}$ in (a) Right handed material, (b) Left handed material.

Moreover, the orientation of the wave vector $\vec{k}$ gives the direction of the phase velocity. Consequently, phase and group velocities will reversed and become antiparallel. Such antiparallel orientation corresponds to so called "backward waves",or"negative group velocity". The medium then is Left Handed. The antiparallelity of phase and group velocities immediately affect Snell's law as explained in Figure (2.2).

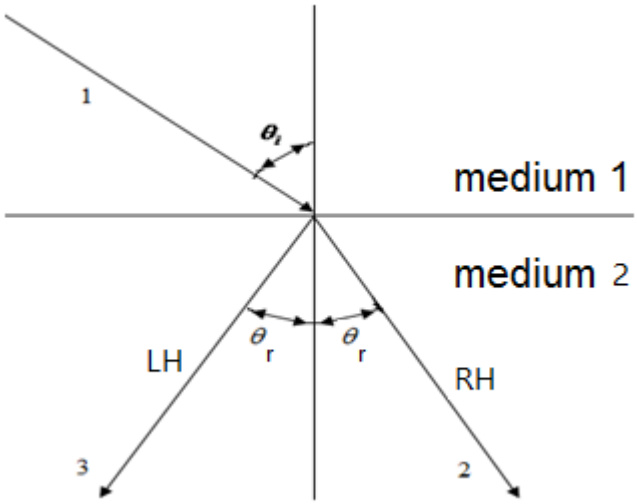

Figure(2.2): Negative refraction of the electromagnetic wave on the interface of a "right-handed" and a "left-handed" material.

The ray propagates along the way (1–2) through the interface between two media for positive values of ε and μ. Otherwise, if one of the media has negative ε and μ, the ray takes the bath (1–3). This unusual propagation of the wave, first discussed by Schuster (Schuster, 1904), is a result of the opposite travelling of the phase and group velocities and of the continuity of the tangential components of the wave vector on the interface between the two media (Markos and Soukoulis, 2008).

2.2.2 Left-Handed medium as a lossy medium

The energy of electromagnetic field is given by (Sarid and Challener, 2010)

$$U = \frac{1}{8\pi}\left\{\frac{\partial(\varepsilon\omega)}{\partial\omega}E^2 + \frac{\partial(\mu\omega)}{\partial\omega}H^2\right\} \tag{2.1}$$

implies that the permittivity ε and permeability μ must depend on the frequency. This dependence means that both the permittivity and permeability must be complex, such as any lossy media. Otherwise, the energy U reduces to the expression $U = \left(\varepsilon E^2 + \mu H^2\right)/(8\pi)$ which would have unacceptable negative value for negative

ε and μ (Markos and Soukoulis, 2008). The general expressions for ε and μ as a function of angular frequency $\omega = 2\pi f$ were proposed as

$$\varepsilon_r = 1 - \frac{\omega_p^2}{\omega^2 + i\gamma\omega} \tag{2.2}$$

$$\mu_r = 1 - \frac{F\omega^2}{\omega^2 - \omega_0^2 + i\omega\Gamma} \tag{2.3}$$

where ω_p, γ, F, and Γ are constants associated with a particular metamaterial in the microwave regime correspond to the electric plasma frequency, the damping factor, the fractional area of the unit cell occupied by the spilt ring resonator (SRR), and the dissipation factor, respectively (Sarid and Challener, 2010).

2.2.3 Unique properties of LHMs

An established slab from a left-handed material with negative permittivity and permeability can be regarded in the same way as a dielectric slab. It is, however beneficial to highlight two special properties of the left-handed slab. First, a planar lens can be investigated at the interface of the vacuum and left-handed medium due to the negative refraction (Markos and Soukoulis, 2008). Second, left-handed slab is able to amplify incoming evanescent waves which offers many applications such as perfect lenses (Koschny, Moussa, and Soukoulis, 2006). This abnormal property makes left-handed materials different in principle from any other known material.

2.2.4 Applications of LHMs.

The unique properties of these metamaterials make them the best candidates for most applications. LHMs can be used in many applications, such as cloaks, antenna, resonators, radome, sensors, absorbers and couplers etc(Gangwar, Paras and Gangwar, 2014). These applications are required for the performance improvement of the material. Cloaking means that electromagnetic field inside the hollow cloak tends to be zero, this makes the region inside the shell disappear. This can be achieved by guiding the electromagnet wave, in another world transforming the coordinate system (Ergin, Stenger, Brenner, Pendry and Wegener. 2010).

Researches concerned on the use of LHMs in directive antenna substrate systems (Chen, Wu, Ran, Grzegorczyk and Kong, 2006;Sui et al, 2005; Wu et al, 2005;). The

problem with the designed antennas in the past is the narrowband operation. It is well known that by Snell's law, if a source is embedded in a substrate that has a small index of refraction compared to air, its rays will be transmitted near the normal of the substrate. The light-weight property of LHMs added benefit to design a wideband directive antenna (Li, Yeo, Mosig and Martin. 2010). Moreover, Zero-indexmetamaterials or LHMs where the effective permittivity and permeability are zero at certain frequencies can be used to achieve a wider frequency band of high directivity. To increase the gain of the antenna, a planar radome were arranged by using seven LHMs structures.

The fabrication of LHMs opens a door for designing sensor with specified sensitivity and enhances the resolution of sensors. These sensors are used in wide variety area such as agriculture and biomedical.

Conventional couplers can achieve strong forward coupling. But to obtain a sufficient coupling level, they require very long physical lengths and very tight spacing between the two lines. To avoid this drawback, LHMs induced the possibility of achieving strong forward coupling with length drastically reduced(Gangwar, Paras and Gangwar, 2014).

2.3 Bi-isotropic and bi-anisotropic media

Isotropic means having the same property in all directions. If the properties of a material are different in various directions, it is said to be anisotropic. Isotropic and anisotropic media become polarized or magnetized by induction of electric or magnetic field , without cross coupling between the two fields. The permittivity and permeability of such media may be either a scalar for isotropic medium or a tensor for anisotropic one ,which has been mentioned in a previous chapter.

On the other hand, a bi-isotropic or bi-anisotropic medium have uniquely cross coupling between the electric and magnetic fields make them becomes both polarized and magnetized by induction of an electric or magnetic field. In order to clarify this phenomenon we introduce the micro helix model shown in Figure(2.3).

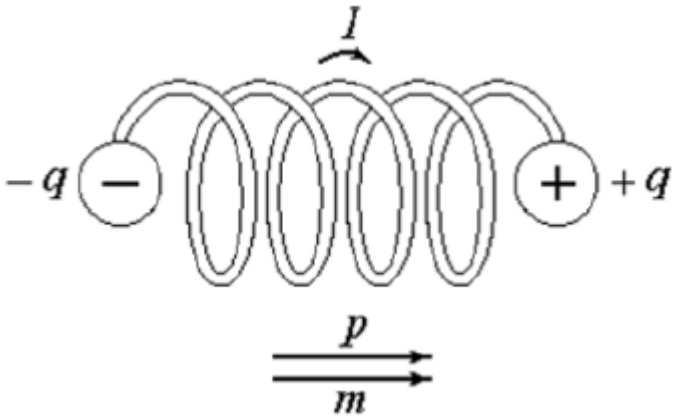

Figure(2.3): micro helix model.

Molecules in isotropic and anisotropic media are considered as electric dipoles and/or current loops. Thus, electric field induced molecules to become aligned electric dipoles and magnetic field induced aligned magnetic dipoles without cross coupling. But in bi-isotropic and bi-anisotropic media, molecules are considered to be a large amount of conductive micro helices shown in Figure (2.3). Aligned electric dipoles (the pair of charges at two ends of the helix) and magnetic dipoles (the current in the helix) appear simultaneously under the action of an electric field or a magnetic field alone. To explain this, charges of opposite signs appear at the two ends of the helix due to the applying of a time-varying electric field and according to the continuous equation current arises in the helix. Moreover, applying of a time-varying magnetic field induced current to arise in the helix according to Lenz's theorem, and again, according to the continuous equation, charges of opposite signs appear at the two ends of the helix. The medium is bi-isotropic if the above phenomenon is isotropic, otherwise it is bi-anisotropic. This kind of media is also known as chiral media (Zhang and Li, 2008). Bi-isotropic and bi-anisotropic media, also called magnetoelectric materials, was theoretically investigated by Landau in 1957 (Zhang and li, 2008). These materials were detected experimentally by Astrov in 1960 in anti-ferromagnetic chromium oxide (In Zhang and li, 2008).

2.3.1 Chiral metamaterials

The Greek word "chiral" means handi.e. our hands are mirror images and they cannot be superimposed on each other, was first predicted by Pasteur (Kim, 2006).

Some magnetic crystal classes are classified among the natural chiral media such as sugar arrays, amino acids, DNA, and organic polymers. Hence, wire helices, the Möbius strip, and the irregular tetrahedron are considered to be artificial chiral objects. A chiral object is three dimensional body which cannot be brought into compatibility with its mirror image by translation and rotation. Such an object has the property of handiness and is either right-handed or left-handed. An object that is not chiral is called achiral(Barba, 2011; Elsherbeni, Demir, Alsharkawy, Arvas and Mahmoud.2004).

To summarize, a chiral medium is a macroscopically continuous medium consists of equivalent uniformly distributed but randomly oriented chiral objects. When a linearly polarized light enters into a slab of chiral medium, it is decomposed into two orthogonal co-propagating circular polarizations, right-handed circulary polarized RCP and left-handed circulary polarized LCP, travelling at different speeds. After propagating through the chiral material and recombining, the output is linearly polarized as well, but is rotated by a certain angle with respect to the plane of polarization of the incident wave (Kim,2006). This rotation depends on the distance travelled through the medium as a result of the optical activity which occurs throughout the medium not at the surface. This property makes a substance able to rotate the plane of incident polarized light due to asymmetrical molecular structure (Bassiri,1987). If the chirality parameter is strong and greater than refractive index at least near the resonant frequency, one eigen-wave in the chiral medium becomes a backward wave and a negative refraction in the chiral medium is generated (Dong, 2009). Therefore, chiral media can achieve negative refraction, we call the type of strong chiral as chiral negative refractive medium (Kim, 2006). Due to the discovery of chiral media and its novel features, recent interest has been focused on the guided structures filled with chiral material, called `chirowaveguides`. Chirowaveguides, first suggested by p. pellet (pellet, 1990), have unique features that the propagation modes are hybrid since the electric and magnetic fields are coupled to each other by chirality.

2.3.2 Previousstudies

Waveguides consisting of chiral metamaterials with negative refractive indices, such as slab, grounded slab, parallel-plate waveguide and fiber, have been investigated theoretically. A special case of chiral negative refractive index medium, termed as chiral nihility in which the permittivity and permeability are simultaneously zero, has also intensively explored. Especially, planar and circular open or closed waveguides containing chiral nihility have been studied. However, these studies focued on the isotropic chiral medium (Dong, 2012).

The wave propagation and field distributions in slab dielectric waveguides having homogenous isotropic chiral material have been discussed by M. Oksanen, P. K. Kolivisto,and I. V. Lindell (1991). The analysis was based on field expansions in the guide and in the upper and lower half spaces. Enforcing the boundary conditions at the waveguide interfaces resulted in eigenvalue equations of the guided modes. Also, the propagation characteristics of general chiral planar waveguides were presented by J. Xiao, K. Zhang, and L. Gong (1997).The eigen equation was given in a simple formulation. The results indicated that there were two types of field distributions which were related to the working wavelength and chiral admittance. Moreover, a waveguide consisting of homogeneous chiral mediain the film and cladding was investigated by M. Yokota and Y. Yamanaka (2006). The electromagnetic fields were decomposed into right and left circularly polarized fields. The guided mode expressions in the film were obtained. Using the boundary conditions at the interfaces yields the eigenvalue equation for the hybrid guided modes. The dispersion relation and the guided mode profile were examined numerically. And, the propagation of electromagnetic plane waves in an isotropic chiral medium was presented by C. W. Qiu, et al. (2008) and a special interest was shown in chiral nihility and the effects of chirality on energy transmission. Some specific case studies of chiral nihility were presented, and Brewster angles were found to cover an extremely wide range. The E-field distributions in these different cases, where the chiral slab was placed in free space, were analyzed by using the appropriate constitutive relations. It was shown from numerical calculations that one can obtain some critical characteristics of the effects of chirality on energy transmission and reflection, such as transparency and power tunneling. The characteristics of guided

modes in a planar waveguides in which the core or cladding consists of chiral nihility meta-materials were studied theoretically by J. Dong and C. Xu (2009). The dispersion curves, electromagnetic fields, energy flow distribution and the power of several low-order guided modes in the chiral nihility waveguides were presented.Also, the characteristics of guided modes in a circular waveguide consisting of uniaxial chiral medium have been investigated by J. F. Dong and J. Li (2012).

2.4 Plane waves in chiral media

If the four tensors appear in the constitutive relations given in Eqs. (1.13) and (1.14) become scalars, the medium is bi-isotropic. Otherwise, the medium is bi-anisotropic . The constitutive relations for this medium were formulated by Tellegen (Tellegen, 1948) as

$$\vec{D} = \varepsilon \vec{E} + \xi \vec{H} \tag{2.4}$$

$$\vec{B} = \zeta \vec{E} + \mu \vec{H} \tag{2.5}$$

$\vec{D}$, $\vec{E}$, $\vec{B}$, $\vec{H}$, ε and μ are corresponding to usual electromagnetic quantities. ξ and ζ are the coupling constants, which is the intrinsic constant of each media can be related to the reciprocity χ and chirality parameter κ as

$$\chi - j\kappa = \frac{\xi}{\sqrt{\varepsilon \mu}} \tag{2.6}$$

$$\chi + j\kappa = \frac{\zeta}{\sqrt{\varepsilon \mu}} \tag{2.7}$$

The chiral medium is reciprocal i.e. $\chi = 0$ .After substitute the above equations into the constitutive relations gives (Dong, 2009)

$$\vec{D} = \varepsilon_i \vec{E} - j\kappa_i \sqrt{\varepsilon_0 \mu_0} \vec{H} \tag{2.8}$$

$$\vec{B} = \mu_i \vec{H} + j\kappa_i \sqrt{\varepsilon_0 \mu_0}\, \vec{E} \tag{2.9}$$

where ε_i and μ_i are the permitivity and permeability of medium i, respectively. κ_i is dimensionless and normalized quantity which represents the handedness of the medium, called the chirality.

2.5 Dispersion equations of three-layered asymmetric slab chiral waveguides

The geometry of an asymmetric slab chiral waveguide with thickness d is shown inFigure(2.4).

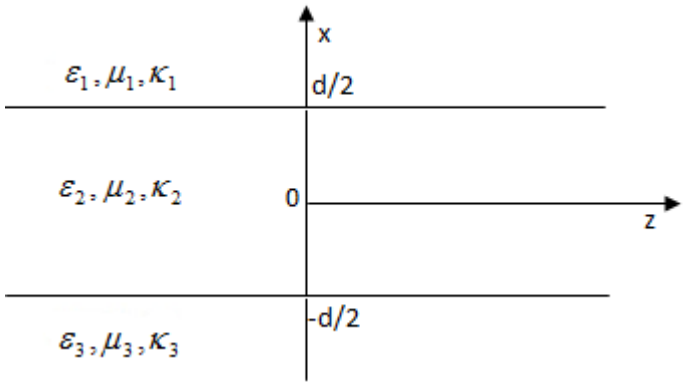

Figure(2.4): Geometry of the three-layered asymmetric slab chiral waveguide.

It consists of a thin chiral meta-material film bounded by isotropic chiral meta-material upper and lower half spaces with different refractive index and chirality. We mentioned that unlike the conventional dielectric materials, the electric and magnetic fields in the chiral material are coupled, so the Hybrid mode appears in the waveguide. This coupling due to the chirality parameter is expressed in the constitutive relations. Depending on which field vectors are used in the relations, the constitutive relations may take different, but equivalent, forms. Eq. (2.8) and Eq. (2.9) coerresponds to the general form of the constitutive relation.

In the chiral medium, electromagnetic fields are expressed as (Dong, 2009)

$$\vec{E} = \vec{E}_+ + \vec{E}_- \tag{2.10}$$

$$\vec{H} = \vec{H}_{+} + \vec{H}_{-} \tag{2.11}$$

The electric and magnetic fields in the chiral medium are related to each other by (Dong, 2009)

$$\vec{H}_{\pm} = \pm \frac{j}{\eta_i} \vec{E}_{\pm} \tag{2.12}$$

where the (±) symbols correspond to the right-handed (RCP) and left-handed (LCP) circularly polarized waves in the chiral material, respectively, and $\eta_i = \sqrt{\mu_i / \varepsilon_i}$ is the wave impedance in the media. After few rearranging of the constitutive relations given in Eq.(2.8) and Eq.(2.9) in the present of Eq. (2.12) one can write

$$\vec{D}_{\pm} = \frac{\varepsilon_i}{n_i} \left(n_i \pm \kappa_i \right) \vec{E}_{\pm} \tag{2.13}$$

Similarly,

$$\vec{B}_{\pm} = \frac{\mu_i}{n_i} \left(n_{\,\mathrm{i}} \pm \kappa_i \right) \vec{H}_{\pm} \tag{2.14}$$

where $n_i = \sqrt{\varepsilon_i \mu_i / \varepsilon_0 \mu_0}$ is the refractive index .

Substitution Eq.(2.13), and Eq.(2.14) into Maxwell's equations for source-free regions leads to a new form for Maxwell's equations

$$\nabla \times \vec{E}_{\pm} = -j\, k_{i\pm}\, \eta_i\, \vec{H}_{\pm} \tag{2.15}$$

$$\nabla \times \vec{H}_{\pm} = j \frac{k_{i\pm}}{\eta_i} \vec{E}_{\pm} \tag{2.16}$$

where $\vec{k}_{i\pm} = k_0(n_i \pm \kappa_i)$ is the wave vector for RCP and LCP waves and $\vec{k}_0 = \omega\sqrt{\varepsilon_0\ \mu_0}$ is the wave vector for free space.

Furthermore, since the structure is uniform in the y direction, we assume $\partial/\partial y = 0$ and the fields are varying with respect to time as $e^{-j(\beta z-\omega t)}$ so we assume $\partial/\partial z = -j\beta$ where β is the propagation constant to be determined.

For better understanding, we again derive the wave equation from Maxwell's equations

$$j\beta\ \vec{E}_{y\pm} = -jk_{i\pm}\ \eta_i\ \vec{H}_{x\pm} \tag{2.17}$$

$$\frac{\partial \vec{E}_{x\pm}}{\partial z} - \frac{\partial \vec{E}_{z\pm}}{\partial x} = -jk_{i\pm}\eta_i\ \vec{H}_{y\pm} \tag{2.18}$$

$$\frac{\partial \vec{E}_{y\pm}}{\partial x} = -jk_{i\pm}\eta_i\ \vec{H}_{z\pm} \tag{2.19}$$

$$j\beta\ \vec{H}_{y\pm} = j\ k_{i\pm}/\eta_i\ \vec{E}_{x\pm} \tag{2.20}$$

$$\frac{\partial \vec{H}_{x\pm}}{\partial z} - \frac{\partial \vec{H}_{z\pm}}{\partial x} = j\,k_{i\pm}/\eta_i\ \vec{E}_{y\pm} \tag{2.21}$$

$$\frac{\partial \vec{H}_{y\pm}}{\partial x} = j\,k_{i\pm}/\eta_i\ \vec{E}_{z\pm} \tag{2.22}$$

The wave equation for the principal electric field component $\vec{E}_y$ is derived as follow

$$\nabla_\perp^2\ \vec{E}_{y\pm} + k_{i\pm}^2\ \vec{E}_{y\pm} = 0 \tag{2.23}$$

We can express the solutions of the longitudinal-field component in Eq. (2.23) as

$$\vec{E}_{z\pm}(x)=\begin{cases}A_{\pm}exp\left(-\gamma_{\pm}\left(x-\frac{d}{2}\right)\right), & \mathrm{x} > d/2,\\ B_{\pm}\sin(\delta_{\pm}x) \quad , & -\mathrm{d}/2 \le \mathrm{x} \le \mathrm{d}/2,\\ C_{\pm}\exp\left(\alpha_{\pm}\left(x+\frac{d}{2}\right)\right), & \mathrm{x} < -d/2.\end{cases} \tag{2.24}$$

for odd guided modes, and

$$\vec{E}_{z\pm}(x)=\begin{cases}A_{\pm}exp\left(-\gamma_{\pm}\left(x-\frac{d}{2}\right)\right), & \mathrm{x} > d/2,\\ B_{\pm}\cos(\delta_{\pm}x) \quad , & -\mathrm{d}/2 \le \mathrm{x} \le \mathrm{d}/2,\\ C_{\pm}\exp\left(\alpha_{\pm}\left(x+\frac{d}{2}\right)\right), & \mathrm{x} < -d/2.\end{cases} \tag{2.25}$$

for even guided modes, where the parameters $\gamma_{\pm}$,$\delta_{\pm}$ and $\alpha_{\pm}$ are given by
$\gamma_{\pm}=(\beta^2-k_{1\pm}^2)^{1/2}$,$\delta_{\pm}=(k_{2\pm}^2-\beta^2)^{1/2}$,$\alpha_{\pm}=(\beta^2-k_{3\pm}^2)^{1/2}$.
The other field components can be obtained by using Eqs. (2.12), (2.19), and (2.20). According to the boundary condition (continuity of the tangential fields) for electromagnetic field components at $x=d/2$ and $x=-d/2$, the dispersion equations of guided modes in slab chiral waveguide can be derived as follow

$$\begin{aligned}&\frac{4\gamma_{+}k_{2+}k_{2-}}{\delta_{-}}\left(\frac{\eta_2-\eta_1}{\eta_3}\right)\cos u_{+}\cos u_{-}+4\left(\frac{\eta_2-\eta_1}{\eta_3}\right)\left(\mathrm{k}_{1+}k_{2+}\right)\sin u_{-}\cos u_{+}+\\ &\gamma_{+}k_{2+}\left(1+\frac{\eta_2}{\eta_3}\right)\left(1-\frac{\eta_2}{\eta_3}\right)\left(1+\frac{\eta_1}{\eta_2}\right)\left(\frac{k_{3-}}{\alpha_{-}}+\frac{k_{3+}}{\alpha_{+}}\right)\sin u_{-}\cos u_{+}-\\ &\left\{\frac{k_{3-}}{\alpha_{-}}\left(1-\frac{\eta_2}{\eta_3}\right)^2+\frac{k_{3+}}{\alpha_{+}}\left(1+\frac{\eta_2}{\eta_3}\right)^2\right\}\left(1-\frac{\eta_1}{\eta_2}\right)\left(\frac{\gamma_{+}\delta_{+}k_{2-}}{\delta_{-}}\right)\cos u_{-}\sin u_{+}-\\ &\left\{2\frac{k_{3-}}{\alpha_{-}}\left(1-\frac{\eta_2}{\eta_3}\right)\left(1+\frac{\eta_1}{\eta_3}\right)+2\frac{k_{3+}}{\alpha_{+}}\left(1+\frac{\eta_2}{\eta_3}\right)\left(1-\frac{\eta_1}{\eta_3}\right)\right\}\delta_{+}k_{1+}\sin u_{+}\sin u_{-}=0\end{aligned} \tag{2.26}$$

for odd guided modes, and

$$-\frac{4\gamma_+ k_{2+}k_{2-}}{\delta_-}\left(\frac{\eta_2-\eta_1}{\eta_3}\right)\sin u_+ \sin u_- + 4\left(\frac{\eta_2-\eta_1}{\eta_3}\right)(k_{1+}k_{2+})\cos u_- \sin u_+ +$$

$$\gamma_+ k_{2+}\left(1+\frac{\eta_2}{\eta_3}\right)\left(1-\frac{\eta_2}{\eta_3}\right)\left(1+\frac{\eta_1}{\eta_2}\right)\left(\frac{k_{3-}}{\alpha_-}+\frac{k_{3+}}{\alpha_+}\right)\cos u_- \sin u_+ -$$

$$\left\{\frac{k_{3-}}{\alpha_-}\left(1-\frac{\eta_2}{\eta_3}\right)^2+\frac{k_{3+}}{\alpha_+}\left(1+\frac{\eta_2}{\eta_3}\right)^2\right\}\left(1-\frac{\eta_1}{\eta_2}\right)\left(\frac{\gamma_+\delta_+ k_{2-}}{\delta_-}\right)\sin u_- \cos u_+ -$$

$$\left\{2\frac{k_{3-}}{\alpha_-}\left(1-\frac{\eta_2}{\eta_3}\right)\left(1+\frac{\eta_1}{\eta_3}\right)+2\frac{k_{3+}}{\alpha_+}\left(1+\frac{\eta_2}{\eta_3}\right)\left(1-\frac{\eta_1}{\eta_3}\right)\right\}\delta_+ k_{1+}\cos u_+ \cos u_- = 0 \qquad (2.27)$$

for even guided modes, where $u_\pm = \delta_\pm d/2$. In the next section we will study the dispersion equations of guided modes in a three-layered symmetric slab chiral waveguide.

2.6 Dispersion equations of a three-layered symmetric slab chiral waveguides

If the chiral meta-materials in the claddings shown in Figure (2.3) have the same refractive index and chirality as those of the substrate; $\kappa_1 = \kappa_3$, $\varepsilon_1 = \varepsilon_3$ and $\mu_1 = \mu_3$, then we have a symmetric three- layered slab chiral waveguide as shown in Figure(2.5).

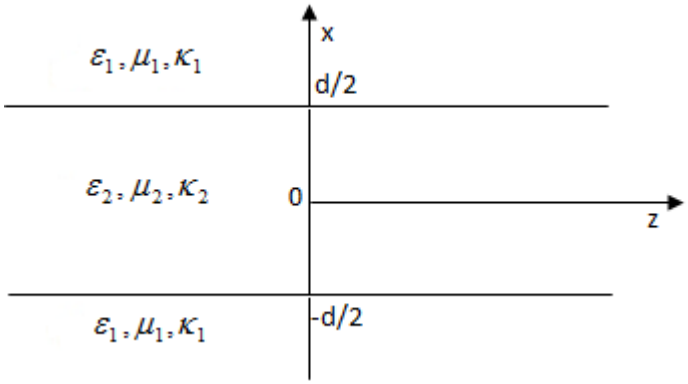

Figure(2.5): Geometry of the three-layered symmetric slab chiral waveguide.

The solutions of the longitudinal-field component in Eq.(2.23) are written as

$$\vec{E}_{z\pm}(x)=\begin{cases}A_{\pm}\exp\left(-\gamma_{\pm}\left(x-\dfrac{d}{2}\right)\right), & \mathrm{x}>d/2,\\ B_{\pm}\sin(\delta_{\pm}x)\ , & -\mathrm{d}/2\le \mathrm{x}\le \mathrm{d}/2,\\ A_{\pm}\exp\left(\gamma_{\pm}\left(x+\dfrac{d}{2}\right)\right), & \mathrm{x}<-d/2.\end{cases} \tag{2.28}$$

for odd guided modes, and

$$\vec{E}_{z\pm}(x)=\begin{cases}A_{\pm}\exp\left(-\gamma_{\pm}\left(x-\dfrac{d}{2}\right)\right), & \mathrm{x}\ge \mathrm{d}/2,\\ B_{\pm}\cos(\delta_{\pm}x)\ , & -\mathrm{d}/2<x<d/2,\\ A_{\pm}\exp\left(\gamma_{\pm}\left(x+\dfrac{d}{2}\right)\right)\ , & \mathrm{x}\le -\mathrm{d}/2.\end{cases} \tag{2.29}$$

for even guided modes.

Other components of the fields are obtained and the continuity requirements are applied, we obtain the following dispersion relations

$$\frac{4k_{2+}k_{2-}}{\delta_{+}\delta_{-}}\cos u_{+}\cos u_{-}+\frac{4k_{1+}k_{1-}}{\gamma_{+}\gamma_{-}}\sin u_{+}\sin u_{-}-$$
$$\left(\frac{1}{\eta_1\eta_2}\right)\begin{Bmatrix}\left(\dfrac{k_{1+}k_{2+}}{\delta_{+}\gamma_{+}}(\eta_1-\eta_2)^2+\dfrac{k_{1-}k_{2+}}{\delta_{+}\gamma_{-}}(\eta_1+\eta_2)^2\right)\sin u_{-}\cos u_{+}+\\ \left(\dfrac{k_{1-}k_{2-}}{\delta_{-}\gamma_{-}}(\eta_1-\eta_2)^2+\dfrac{k_{1+}k_{2-}}{\delta_{-}\gamma_{+}}(\eta_1+\eta_2)^2\right)\cos u_{-}\sin u_{+}\end{Bmatrix}=0 \tag{2.30}$$

for odd guided modes, and

$$\frac{4k_{1+}k_{1-}}{\gamma_+\gamma_-}\cos u_+\cos u_- + \frac{4k_{2+}k_{2-}}{\delta_+\delta_-}\sin u_+\sin u_- +$$

$$\left(\frac{1}{\eta_1\eta_2}\right)\left\{\begin{array}{l}\left(\dfrac{k_{1-}k_{2-}}{\delta_-\gamma_-}(\eta_1-\eta_2)^2+\dfrac{k_{1+}k_{2-}}{\delta_-\gamma_+}(\eta_1+\eta_2)^2\right)\sin u_-\cos u_+ + \\ \left(\dfrac{k_{1+}k_{2+}}{\delta_+\gamma_+}(\eta_1-\eta_2)^2+\dfrac{k_{1-}k_{2+}}{\delta_+\gamma_-}(\eta_1+\eta_2)^2\right)\cos u_-\sin u_+\end{array}\right\}=0 \qquad (2.31)$$

for even guided modes.

Chapter 3

Characteristics of Electromagnetic Waves in Slab Waveguide Structures Comprising Chiral Nihility Film and Left-Handed Material Claddings.

Chapter 3

Characteristics of Electromagnetic Waves in Slab Waveguide Structures Comprising ChiralNihilityFilm and Left-Handed Material Claddings.

Weanalytically present the dispersion equationfor a symmetric three-layered chiro-waveguides, in which the claddings are achiral material but the core is chiral material. After that,two modes of propagation through a chiral nihility core and left handed material (LHM) claddings waveguide are treated in details. For odd and even guided modes, the dispersion equations, normalized cutoff frequencies, electromagnetic fields, and energy flow of right-handed and left-handed circularly polarized (RCP and LCP) modes are derived in explicit forms. Numerical results of guided low-order modes and typical chirality parameters are given. Some novel features such as abnormal dispersion curves are found.

3.1 Dispersion equations of three-layered symmetric slab chiral core and achiral claddings waveguides

When the waveguide shown in Figure (2.5) consists of a chiral core and an achiral claddings, where $\kappa_1 = 0$, as shown in Figure (3.1), the above parameters $\vec{k}_{i\pm} = k_0(n_i \pm \kappa_i)$,$\gamma_\pm = (\beta^2 - k_{1\pm}^2)^{1/2}$,$\delta_\pm = (k_{2\pm}^2 - \beta^2)^{1/2}$and $\alpha_\pm = (\beta^2 - k_{3\pm}^2)^{\frac{1}{2}}$become$k_{1\pm} = n_1 k_0 = k_1$,$k_{2\pm} = k_0(n_2 \pm \kappa_2)$,$\gamma_\pm = (\beta^2 - k_1^2)^{\frac{1}{2}} = \gamma$,$\delta_\pm = (k_{2\pm}^2 - \beta^2)^{1/2}$.

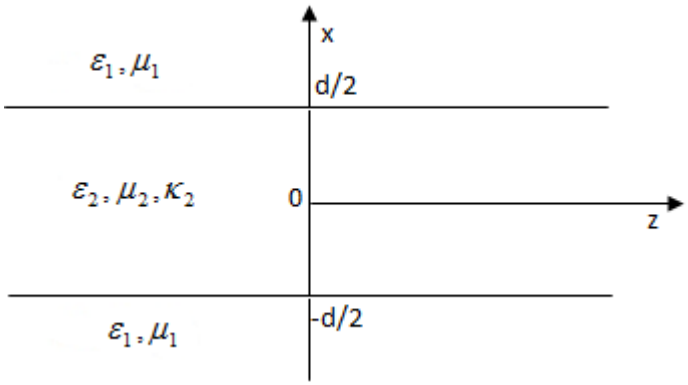

Figure(3.1): Geometry of the three-layered symmetric slab chiral core and achiral claddings waveguide.

The dispersion equations (2.30), (2.31) reduce to

$$\frac{2k_0^2(n_2^2-\kappa_2^2)}{\delta_+\delta_-}\cos u_+\cos u_- + \frac{2k_1^2}{\gamma^2}\sin u_+\sin u_- - \frac{k_1(\eta_1^2+\eta_2^2)}{\gamma\eta_1\eta_2}\left\{\frac{k_{2+}}{\delta_+}\sin u_-\cos u_+ + \frac{k_{2-}}{\delta_-}\cos u_-\sin u_+\right\}=0 \tag{3.1}$$

for odd guided modes, and

$$\frac{2k_1^2}{\gamma^2}\cos u_+\cos u_- + \frac{2k_0^2(n_2^2-\kappa_2^2)}{\delta_+\delta_-}\sin u_+\sin u_- + \frac{k_1(\eta_1^2+\eta_2^2)}{\gamma\eta_1\eta_2}\left\{\frac{k_{2+}}{\delta_+}\cos u_-\sin u_+ + \frac{k_{2-}}{\delta_-}\sin u_-\cos u_+\right\}=0 \tag{3.2}$$

for even guided modes.

When the core is a chiral nihility meta-material, in which the permittivity and permeability are simultaneously zero, the above parameters become $k_{1\pm} = n_1 k_0 = k_1, k_{2\pm} = \pm k_0\kappa_2, \gamma_\pm = (\beta^2 - k_1^2)^{\frac{1}{2}} = \gamma, \delta_\pm = (k_{2\pm}^2 - \beta^2)^{\frac{1}{2}} = (k_0^2\kappa_2^2 - \beta^2)^{1/2} = \delta$

The dispersion relation given by Eq. (3.1) can be divided into two equations as

$$(k_0^2\kappa_2^2 - \beta^2)^{\frac{1}{2}}\frac{d}{2} = tan^{-1}\{\frac{k_0\kappa_2}{k_1}(\frac{\beta^2 - k_1^2}{k_0^2\kappa_2^2 - \beta^2})^{\frac{1}{2}}\} + m\pi, \qquad m = 0,1,2,\ldots \tag{3.3}$$

for RCP odd modes, and

$$(k_0^2\kappa_2^2-\beta^2)^{\frac{1}{2}}\frac{d}{2}=-tan^{-1}\{\frac{k_0\kappa_2}{k_1}(\frac{\beta^2-k_1^2}{k_0^2\kappa_2^2-\beta^2})^{\frac{1}{2}}\}+m\pi,\qquad m=1,2,3,\ldots \tag{3.4}$$

for LCP odd modes, where m is mode number. It is noted that m starts from 0 in RCP odd modes and from 1 in LCP odd modes.

Moreover, the dispersion relation given by Eq. (3.2) can also be divided into two equations, taking in mind that RCP and LCP even guided modes are mirror images of RCP and LCP odd guided modes, then the dispersion equations take the form

$$(k_0^2\kappa_2^2-\beta^2)^{\frac{1}{2}}\frac{d}{2}=-tan^{-1}\{\frac{k_1}{k_0\kappa_2}(\frac{k_0^2\kappa_2^2-\beta^2}{\beta^2-k_1^2})^{\frac{1}{2}}\}+m\pi,\qquad m=1,2,3,\ldots \tag{3.5}$$

for RCP even modes, and

$$(k_0^2\kappa_2^2-\beta^2)^{\frac{1}{2}}\frac{d}{2}=tan^{-1}\{\frac{k_1}{k_0\kappa_2}(\frac{k_0^2\kappa_2^2-\beta^2}{\beta^2-k_1^2})^{\frac{1}{2}}\}+m\pi,\qquad m=0,1,2,\ldots \tag{3.6}$$

for LCP even modes. It is noted that, in contrast to odd modes, m starts from 1 in RCP odd modes and from 0 in LCP odd modes, because of the handedness of chiral meta-material.

3.2 Guided modes in slab chiral nihility core and LHMs claddings waveguides

Consider the structure shown in Figure (3.1) with chiral nihility core and the claddings are left-handed material. It is shown that the dispersion relation given by Eq. (3.1) and Eq. (3.2) can be divided into two equations corresponding to RCP and LCP modes, respectively. For odd and even guided modes, the dispersion equations, normalized cut-off frequencies, electromagnetic fields, and energy flow of RCP and LCP modes are found as follows.

3.2.1 Odd modes

We use in the claddings left-handed materials (LHMs), which, by definition, have a negative refractive index. The parameter n_1 have a negative value, so the dispersion relation given by Eq. (3.1) is divided into two equations as

$$(k_0^2\kappa_2^2 - \beta^2)^{\frac{1}{2}}\frac{d}{2} = tan^{-1}\{\frac{k_0\kappa_2}{k_1}(\frac{\beta^2 - k_1^2}{k_0^2\kappa_2^2 - \beta^2})^{\frac{1}{2}}\} + m\pi, \qquad m = 1,2,3,\ldots \tag{3.7}$$

for RCP odd modes, and

$$(k_0^2\kappa_2^2 - \beta^2)^{\frac{1}{2}}\frac{d}{2} = -tan^{-1}\{\frac{k_0\kappa_2}{k_1}(\frac{\beta^2 - k_1^2}{k_0^2\kappa_2^2 - \beta^2})^{\frac{1}{2}}\} + m\pi, \qquad m = 0,1,2,\ldots \tag{3.8}$$

for LCP odd modes. It is noted that, in contrast to Eqs (3.3) and (3.4), m starts from 0 in LCP odd modes and from 1 in RCP odd modes.

We can obtain the normalized cutoff frequencies (V) by setting $\beta \to k_1$ in the dispersion Equations (3.7) and (3.8)

$$V = k_0 d = \frac{2m\pi}{(\kappa_2^2 - n_1^2)^{1/2}}, \qquad m = 1,2,3,\ldots \tag{3.9}$$

for RCP odd modes, and

$$V = k_0 d = \frac{2m\pi}{(\kappa_2^2 - n_1^2)^{1/2}}, \qquad m = 0,1,2,\ldots \tag{3.10}$$

for LCP odd modes.

We can express the electromagnetic fields in explicit forms as

$$E_x(x) = \begin{cases} -\frac{j\beta A}{\gamma}\exp\left\{-\gamma\left(x-\frac{d}{2}\right)\right\} & \mathrm{x} > d/2, \\ -\frac{j\beta A}{\delta\sin(u)}\cos(\delta x) & -\mathrm{d}/2 \le \mathrm{x} \le \mathrm{d}/2, \\ +\frac{j\beta A}{\gamma}\exp\left\{\gamma\left(x+\frac{d}{2}\right)\right\} & \mathrm{x} < -d/2. \end{cases} \tag{3.11}$$

$$E_y(x) = \begin{cases} \mp\frac{k_1 A}{\gamma}\exp\left\{-\gamma\left(x-\frac{d}{2}\right)\right\} & \mathrm{x} > d/2, \\ -\frac{k_0\kappa_2 A}{\delta\sin(u)}\cos(\delta x) & -\mathrm{d}/2 \le \mathrm{x} \le \mathrm{d}/2, \\ \pm\frac{k_1 A}{\gamma}\exp\left\{\gamma\left(x+\frac{d}{2}\right)\right\} & \mathrm{x} < -d/2. \end{cases} \tag{3.12}$$

and

$$E_z(x) = \begin{cases} A\exp\{-\gamma(x-d/2)\} & \mathrm{x} > d/2, \\ \frac{A}{\sin(u)}\sin(\delta x) & -\mathrm{d}/2 \le \mathrm{x} \le \mathrm{d}/2, \\ A\exp\{\gamma(x+d/2)\} & \mathrm{x} < -d/2. \end{cases} \tag{3.13}$$

for RCP (upper sign) and LCP (lower sign) odd modes, respectively where A is an arbitrary constant, which can be determined by total power.

The magnetic fields in the core and the claddings are

$$H_{\mathrm{x,y,z}} = \pm\frac{\mathrm{j}}{\eta_1} E_{\mathrm{x,y,z}} \tag{3.14}$$

for RCP (upper sign) and LCP (lower sign) odd modes, respectively.

Energy flow along the z-axis in the waveguides is defined by

$$S_z = \frac{1}{2} Re(E \times H^*) = \frac{1}{2} Re(E_x H_y^* - E_y H_x^*) \tag{3.15}$$

Thus we can express enery flow along the z-axis as

$$S_z(x) = \begin{cases} \dfrac{\beta k_1 A^2}{\eta_1 \gamma^2} exp\left\{-2\gamma\left(x - \dfrac{d}{2}\right)\right\} & \text{x} > d/2, \\ \pm \dfrac{\beta k_0 \kappa_2 A^2}{\eta_1 \delta^2 \sin^2(u)} \cos^2(\delta x) & -\text{d}/2 \le \text{x} \le \text{d}/2, \\ \dfrac{\beta k_1 A^2}{\eta_1 \gamma^2} \exp\left\{2\gamma\left(x + \dfrac{d}{2}\right)\right\} & \text{x} < -d/2. \end{cases} \tag{3.16}$$

for RCP (upper sign) and LCP (lower sign) odd modes, respectively.

It is obvious from Eq.(3.16) that S_z is positive for RCP odd modes and negative for LCP odd modes in the core, and positive for both RCP and LCP odd modes in the claddings. On the other hand, we use LHM claddings which make the energy flux negative in the claddings for both RCP and LCP odd modes.

3.2.2 Even modes

When the claddings are left-handed materials (LHMs) and the indexn_1 have a negative value, the dispersion equation (3.2) divided into two equations as

$$(k_0^2\kappa_2^2 - \beta^2)^{\frac{1}{2}} \frac{d}{2} = -tan^{-1}\{\frac{k_1}{k_0\kappa_2}(\frac{k_0^2\kappa_2^2 - \beta^2}{\beta^2 - k_1^2})^{\frac{1}{2}}\} + m\pi, \qquad m = 0,1,2,\ldots \tag{3.17}$$

for RCP even modes, and

$$(k_0^2\kappa_2^2 - \beta^2)^{\frac{1}{2}} \frac{d}{2} = \ tan^{-1}\{\frac{k_1}{k_0\kappa_2}(\frac{k_0^2\kappa_2^2 - \beta^2}{\beta^2 - k_1^2})^{\frac{1}{2}}\} + m\pi, m = 1,2,3,\ldots \tag{3.18}$$

for LCP even modes.

We can obtain the normalized cutoff frequencies (V) by setting $\beta \to \kappa_1$ in the dispersion Equations (3.17) and (3.18):

$$V = k_0 d = \frac{(2m+1)\pi}{(\kappa_2^2 - n_1^2)^{1/2}}, m = 0,1,2,\ldots \tag{3.19}$$

for RCP even modes, and

$$V = k_0 d = \frac{(2m-1)\pi}{(\kappa_2^2 - n_1^2)^{1/2}}, m = 1,2,3,\ldots \tag{3.20}$$

for LCP even modes.

We can express the electromagnetic fields in explicit forms as

$$E_x(x) = \begin{cases} -\frac{j\beta A}{\gamma} exp\left\{-\gamma\left(x - \frac{d}{2}\right)\right\} & \mathrm{x} > d/2, \\ +\frac{j\beta A}{\delta \cos(u)} \sin(\delta x) & -\mathrm{d}/2 \le \mathrm{x} \le \mathrm{d}/2, \\ +\frac{j\beta A}{\gamma} \exp\left\{\gamma\left(x + \frac{d}{2}\right)\right\} & \mathrm{x} < -d/2. \end{cases} \tag{3.21}$$

$$E_y(x) = \begin{cases} \mp\frac{k_1 A}{\gamma} exp\left\{-\gamma\left(x - \frac{d}{2}\right)\right\} & \mathrm{x} > d/2, \\ +\frac{k_0 \kappa_2 A}{\delta \cos(u)} \sin(\delta x) & -\mathrm{d}/2 \le \mathrm{x} \le \mathrm{d}/2, \\ \pm\frac{k_1 A}{\gamma} \exp\left\{\gamma\left(x + \frac{d}{2}\right)\right\} & \mathrm{x} < -d/2. \end{cases} \tag{3.22}$$

and

$$E_z(x) = \begin{cases} Aexp\left\{-\gamma\left(x - \frac{d}{2}\right)\right\} & \text{x} > d/2, \\ \frac{A}{\cos(u)}\cos(\delta x) & -\text{d}/2 \le \text{x} \le \text{d}/2, \\ A\exp\left\{\gamma\left(x + \frac{d}{2}\right)\right\} & \text{x} < -d/2. \end{cases} \quad (3.23)$$

for RCP (upper sign) and LCP (lower sign) even modes, respectively.
The magnetic fields in the core and the claddings are given by Eq.(3.14).
Moreover, we can express the enery flow along the z-axis in the waveguide as

$$S_z(x) = \begin{cases} \frac{\beta k_1 A^2}{\eta_1 \gamma^2} exp\left\{-2\gamma\left(x - \frac{d}{2}\right)\right\} & \text{x} > d/2, \\ \pm\frac{\beta k_0 \kappa_2 A^2}{\eta_1 \delta^2 \cos^2(u)}\sin^2(\delta x) & -\text{d}/2 \le \text{x} \le \text{d}/2, \\ \frac{\beta k_1 A^2}{\eta_1 \gamma^2}\exp\left\{2\gamma\left(x + \frac{d}{2}\right)\right\} & \text{x} < -d/2. \end{cases} \quad (3.24)$$

for RCP (upper sign) and LCP (lower sign) even modes, respectively.
ALso, it is obvious from Eq.(3.24) that S_z is positive for RCP even modes and negative for LCP even modes in the core, and positive for both RCP and LCP even modes in the claddings. On the other hand, we use LHM claddings which make the energy flux negative in the claddings for both RCP and LCP even modes.

3.3 Results and discusion

We can calculate the propagation constants numerically from the dispersion equations (3.7), (3.8), (3.17) and (3.18), then the electromagnetic fields and the energy flow distribution can be calculated.
In this section, we assume chiral nihility core guiding film with the parameters $\mu_2 = \varepsilon_2 = 0, \kappa_2 = 1.5$. On the other hand, the cladding and substrate are LHMs with parameters$\mu_1 = (-1 + .001\,\text{I}) \times \mu_0, \varepsilon_1 = (-1 + .001\,\text{I}) \times \varepsilon_0$, and $\kappa_1 = 0$.

3.3.1 Dispersion curves

Figure (3.2) shows the dispersion curves of odd and even guided modes in the slab chiral nihility core and LHMs claddings waveguide for low-order modes, where $n_{eff} = \beta/k_0$ is the effective refractive index, $k_0 d$ is the normalized frequency. Dashed and solid curves related to the odd and even modes, respectively. For LCP odd and even modes, the curves of effective refractive index versus normalized frequency increases monotonically, and the normalized cutoff frequencies (points C_1, C_2 when $n_{eff} = 1$) satisfy Eq.(3.10) or Eq.(3.20). However, for RCP odd and even modes, dispersion curves are no longer increasing monotonically, but are bent, and the cutoff frequencies where $n_{eff} = 1$ are not the minimum frequencies that waves can propagate. When $m = 0$, there is one solution below cutoff frequency (pointC_1) for RCP even mode in some frequency region. When $m = 1$, there are two solutions below cutoff frequencies (points C_2, C_3) for both RCP even and odd modes in some frequency region. Thus the cutoff frequencies here are not really "cutoff". The real "cutoff" frequencies correspond to the minimum frequencies (critical points B, D) that guided wave can propagate. As the normalized frequency increases from the critical points B, D dispersion curves bifurcate two branches, which the effective refractive index increases for upper branch and decreases to $n_{eff} = 1$ for lower branch.

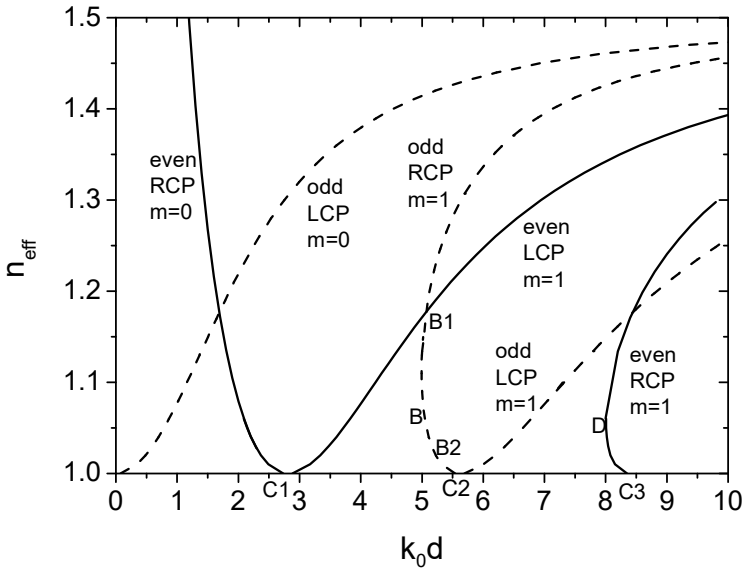

Figure(3.2): Dispersion curves of guided modes in the slab chiral nihility core and LHM claddings waveguide.

3.3.2 Odd guided modes

Figures (3.3) and (3.4) show the amplitudes of electromagnetic field components and energy flux distribution at normalized frequency $k_0 d = 5.2$ for RCP odd mode when m=1. E_z, H_z are odd functions of x (sin form) and E_x, E_y, H_x, H_y (cos form) are even functions of x. S_z is positive in the core and is negative in the claddings (due to the negative refractive index of LHM claddings). However, there are two propagation constants at $k_0 d = 5.2$.

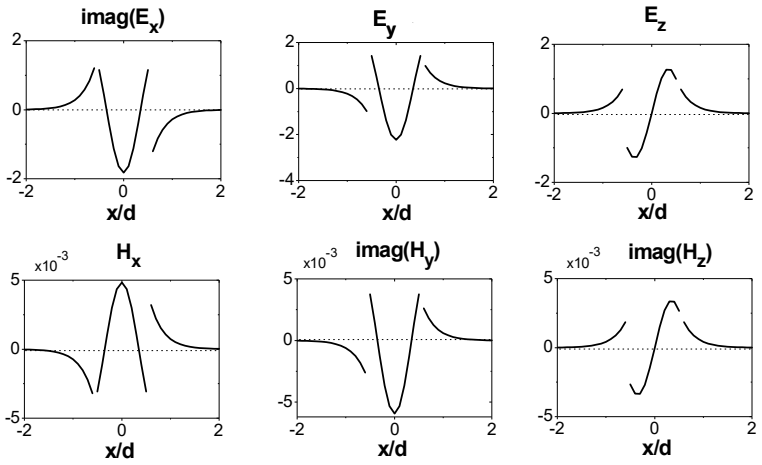

Figure(3.3): Amplitudes of electromagnetic field components at $k_0 d = 5.2$ for RCP odd mode when m=1,$n_{eff} = 1.223$.

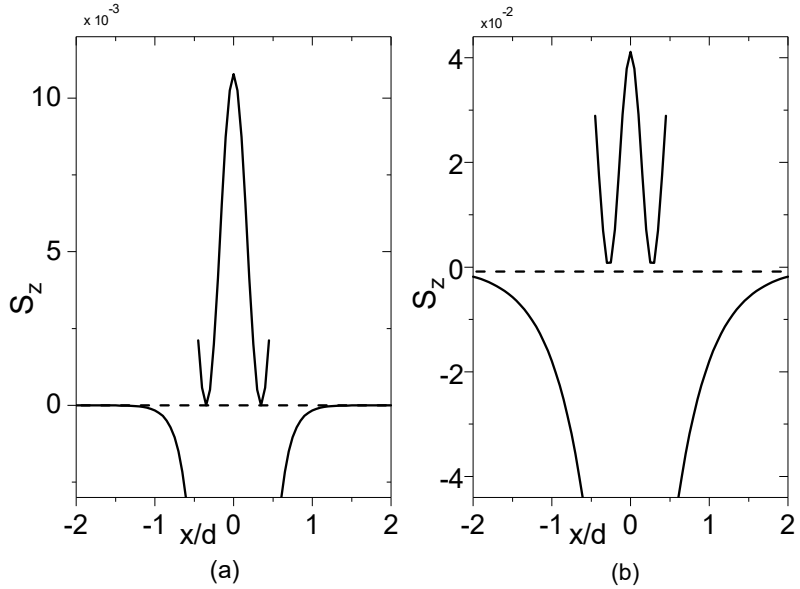

Figure(3.4): Energy flux at $k_0 d = 5.2$ for RCP odd mode when m=1, (a)$n_{eff} = 1.223$; (b) $n_{eff} = 1.02219$.

Figures (3.5) and (3.6) show the amplitudes of electromagnetic field components and energy flux distribution at normalized frequency $k_0 d = 4$ for LCP odd mode when m=0. E_z, H_z are odd functions of x (sin form) and E_x, E_y, H_x, H_y (cos form)

are even functions of x. S_z is negative in both the core and the claddings (due to the negative refractive index of LHM claddings).

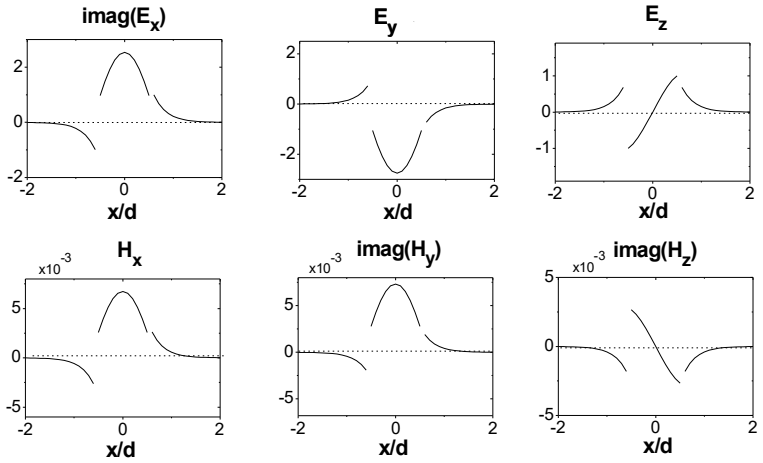

Figure(3.5): Amplitudes of electromagnetic field components at $k_0 d = 4$ for LCP odd mode when m=0.

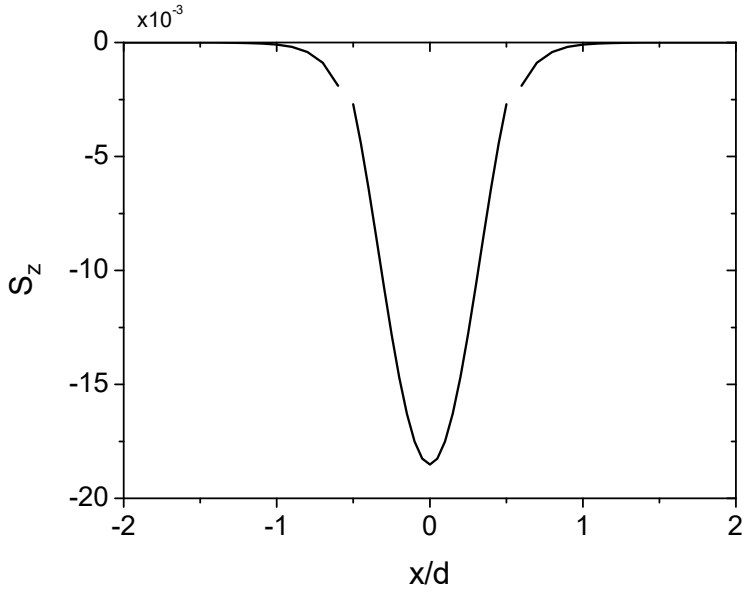

Figure(3.6): Energy flux at $k_0 d = 4$ for LCP odd mode when m=0.

3.3.3. Even guided modes

Figures (3.7) and (3.8) show the amplitudes of electromagnetic field components and energy flux distribution at normalized frequency $k_0 d = 1.5$ for RCP even mode when m=0. E_z, H_z are even functions of x(cos form) and E_x, E_y, H_x, H_y (sin form) are odd functions of x. S_z is positive in the core and is negative the claddings (due to the negative refractive index of LHM claddings).

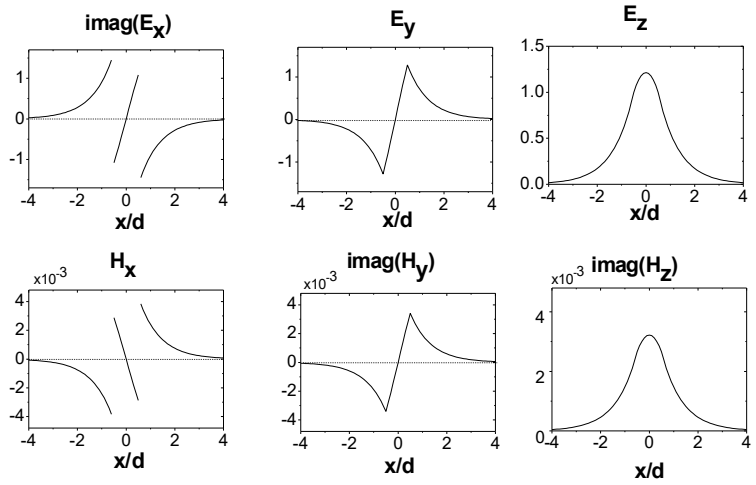

Figure(3.7): Amplitudes of electromagnetic field components at $k_0 d = 1.5$ for RCP even mode when m=0.

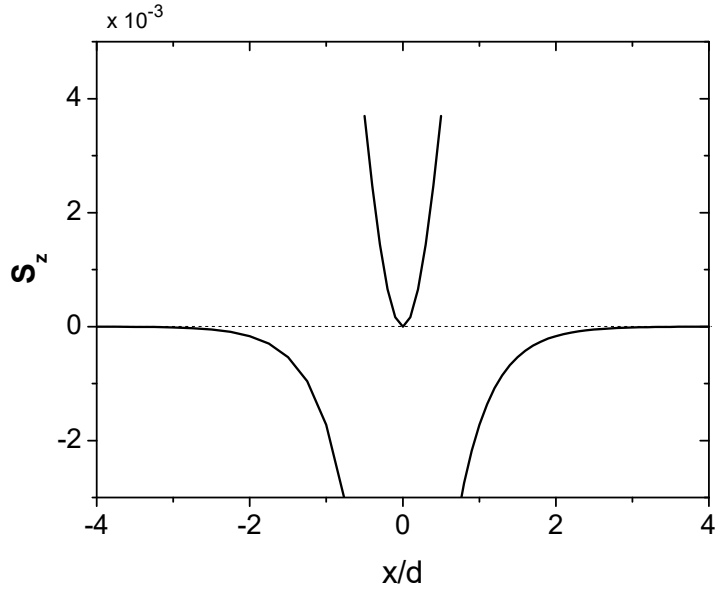

Figure(3.8): Energy flux at $k_0 d = 1.5$ for RCP even mode when m=0.

Figures (3.9) and (3.10) show the amplitudes of electromagnetic field components and energy flux distribution at normalized frequency $k_0 d = 6$ for LCP even mode when m=1. E_z, H_z are even functions of x (cos form) and E_x, E_y, H_x, H_y (sin form) are odd functions of x. S_z is negative in both the core and the claddings (due to the negative refractive index of LHM claddings).

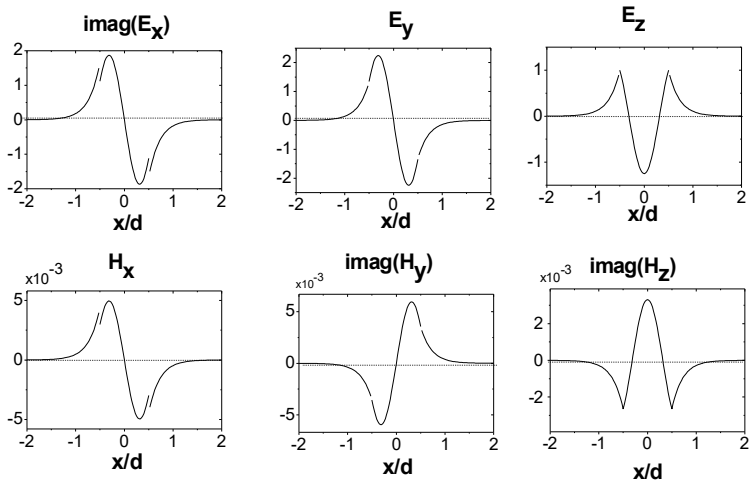

Figure(3.9): Amplitudes of electromagnetic field components at $k_0 d = 6$ for LCP even mode when m=1.

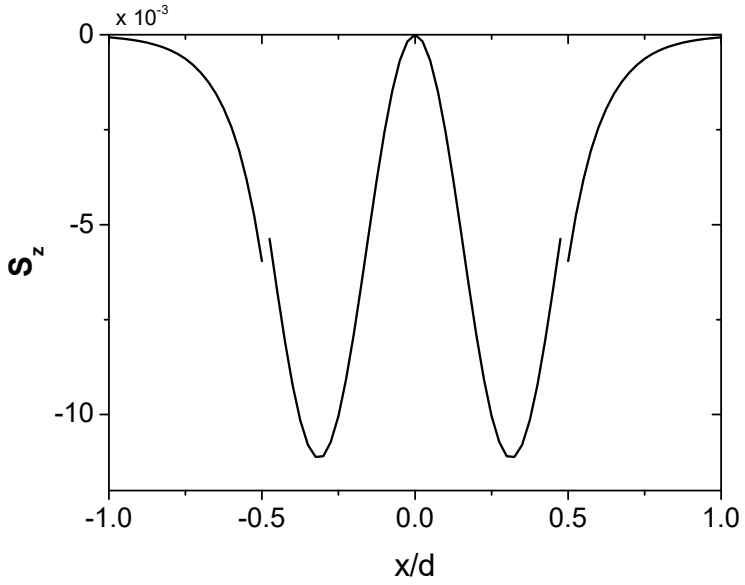

Figure(3.10): Energy flux at $k_0 d = 6$ for LCP even mode when m=1.

Chapter 4

Propagation of Electromagnetic Waves in Slab Waveguide Structure Consisting of Chiral Nihility Claddings and Left-Handed Material Core Layer

Chapter 4

Propagation of Electromagnetic Waves in Slab Waveguide Structure Consisting of Chiral NihilityCladdings and Left-HandedMaterial Core Layer

We derive the dispersion equationfor a symmetric three-layered chiro-waveguides, in which the claddings are chiral material but the core is an achiral material. After that,two modes of propagation through a chiral nihility claddings and left handed material (LHM) core waveguide are presented in details. For odd and even guided modes, the dispersion equations, normalized cutoff frequencies, electromagnetic fields, and energy flow of right-handed and left-handed circularly polarized (RCP and LCP) modes are derived in explicit forms. Numerical results of guided low-order modes and typical chirality parameters are given. Some novel features such as abnormal dispersion curves are found.

4.1 Dispersion relations of three-layered symmetric slab achiral core and chiral cladding waveguides

When the geometry of the waveguide consists of an achiral core and chiral claddings, where$\kappa_2 = 0$, as shown in Figure(4.1) the above parameters become $k_{1\pm} = k_0(n_1 \pm \kappa_1)$, $k_{2\pm} = n_2 k_0 = k_2$, $\gamma_\pm = (\beta^2 - k_{1\pm}^2)^{\frac{1}{2}}$, and$\delta_\pm = (k_2^2 - \beta^2)^{\frac{1}{2}} = \delta$.

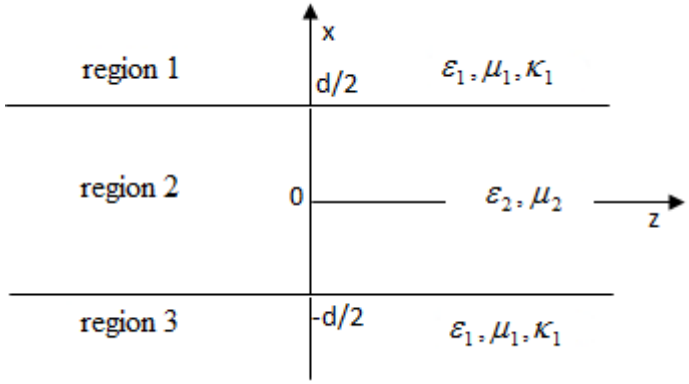

Figure(4.1): Geometry of the three-layered symmetric slab achiral core and chiral cladding waveguide.

The characteristic equations (2.30) and (2.31) can be written as

$$\frac{2k_0^2(n_1^2-\kappa_1^2)}{\gamma_+\gamma_-}\sin^2 u+\frac{2k_2^2}{\delta^2}\cos^2 u-\frac{k_2(\eta_1^2+\eta_2^2)}{\delta\eta_1\eta_2}\sin u\cos u\left\{\frac{\mathrm{k}_{1+}}{\gamma_+}+\frac{k_{1-}}{\gamma_-}\right\}=0 \tag{4.1}$$

for odd guided modes, and

$$\frac{2k_0^2(n_1^2-\kappa_1^2)}{\gamma_+\gamma_-}\cos^2 u+\frac{2k_2^2}{\delta^2}\sin^2 u+\frac{k_2(\eta_1^2+\eta_2^2)}{\delta\eta_1\eta_2}\sin u\cos u\left\{\frac{\mathrm{k}_{1+}}{\gamma_+}+\frac{k_{1-}}{\gamma_-}\right\}=0 \tag{4.2}$$

for even guided modes.

When the claddings are chiral nihility media, in which the permittivity and permeability tend to be zero, the above parameters become $\mathrm{k}_{1\pm}=\pm k_0\kappa_1$, $k_{2\pm}=\mathrm{n}_2\mathrm{k}_0=\mathrm{k}_2$, $\gamma_\pm=(\beta^2-k_{1\pm}^2)^{\frac{1}{2}}=(\beta^2-k_0^2\kappa_1^2)^{\frac{1}{2}}=\gamma$, and$\delta_\pm=(k_2^2-\beta^2)^{\frac{1}{2}}=\delta$. The dispersion relation given in Eq. (4.1) is divided into two equations as

$$(k_2^2-\beta^2)^{\frac{1}{2}}\frac{d}{2}=tan^{-1}\{\frac{k_2}{k_0\kappa_1}(\frac{\beta^2-k_0^2\kappa_1^2}{k_2^2-\beta^2})^{\frac{1}{2}}\}+m\pi,\qquad m=0,1,2,\ldots \tag{4.3}$$

for RCP odd modes, and

$$(k_2^2-\beta^2)^{\frac{1}{2}}\frac{d}{2}=-tan^{-1}\{\frac{k_2}{k_0\kappa_1}(\frac{\beta^2-k_0^2\kappa_1^2}{k_2^2-\beta^2})^{\frac{1}{2}}\}+m\pi,\qquad m=1,2,3,\ldots \tag{4.4}$$

for LCP odd modes, where m is mode number. As can be seen$m$ starts from 0 in RCP odd modes and from 1 in LCP odd modes.

Also, the dispersion relation given in Eq. (4.2) is divided into two equationswhich take the form

$$(k_2^2-\beta^2)^{\frac{1}{2}}\frac{d}{2}=-tan^{-1}\{\frac{k_0\kappa_1}{k_2}(\frac{k_2^2-\beta^2}{\beta^2-k_0^2\kappa_1^2})^{\frac{1}{2}}\}+m\pi,\qquad m=1,2,3,\ldots \tag{4.5}$$

for RCP even modes, and

$$(k_2^2-\beta^2)^{\frac{1}{2}}\frac{d}{2}=tan^{-1}\{\frac{k_0\kappa_1}{k_2}(\frac{k_2^2-\beta^2}{\beta^2-k_0^2\kappa_1^2})^{\frac{1}{2}}\}+m\pi, m=0,1,2,\ldots \quad (4.6)$$

for LCP even modes.As can be seen, in contrast to odd modes, m starts from 1 in RCP odd modes and from 0 in LCP odd modes.

4.2 Guided modes in chiral nihility claddings and NIM core waveguide

Consider region 1 and region 3 shown in Fig.4.1 are chiral nihility material and the core is LHM. It is presented that the dispersion Equations (4.1) and (4.2) can be divided into two equations correspond to RCP and LCP modes. For odd and even guided modes, the dispersion equations, normalized cut-off frequencies, electromagnetic fields,and energy flow of RCP and LCP modes are found as follows.

4.2.1 Odd modes

Assume the core layer is left-handed material, thus the parameter n_2 has a negative value, so the dispersion relation given by Eq. (4.1) can be divided into two equations as

$$(k_2^2-\beta^2)^{\frac{1}{2}}\frac{d}{2}=tan^{-1}\{\frac{k_2}{k_0\kappa_1}(\frac{\beta^2-k_0^2\kappa_1^2}{k_2^2-\beta^2})^{\frac{1}{2}}\}+m\pi, \qquad m=1,2,3,\ldots \quad (4.7)$$

for RCP odd modes, and

$$(k_2^2-\beta^2)^{\frac{1}{2}}\frac{d}{2}=-tan^{-1}\{\frac{k_2}{k_0\kappa_1}(\frac{\beta^2-k_0^2\kappa_1^2}{k_2^2-\beta^2})^{\frac{1}{2}}\}+m\pi, \qquad m=0,1,2\ldots \quad (4.8)$$

for LCP odd modes. It is noted that, in contrast to Eqs. (4.3) and (4.4), m starts from 0 in LCP odd modes and from 1 in RCP odd modes.

We can obtain the normalized cutoff frequencies (V) by setting $\beta \to k_0\kappa_1$ in the dispersion relations (4.7) and (4.8)

$$V = k_0 d = \frac{2m\pi}{(n_2^2 - \kappa_1^2\ )^{1/2}}, \qquad m = 1, 2, 3, \ldots \tag{4.9}$$

for RCP odd modes, and

$$V = k_0 d = \frac{2m\pi}{(n_2^2 - \kappa_1^2\ )^{1/2}}, \qquad m = 0, 1, 2, \ldots \tag{4.10}$$

for LCP odd modes.

We can express the electromagnetic fields in explicit forms as

$$E_x(x) = \begin{cases} -\dfrac{j\beta A \sin(u)}{\gamma} \exp\left\{-\gamma\left(x - \dfrac{d}{2}\right)\right\} & x > d/2, \\ -\dfrac{j\beta A}{\delta} \cos(\delta x) & -d/2 \le x \le d/2, \\ +\dfrac{j\beta A \sin(u)}{\gamma} \exp\left\{\gamma\left(x + \dfrac{d}{2}\right)\right\} & x < -d/2. \end{cases} \tag{4.11}$$

$$E_y(x) = \begin{cases} -\dfrac{k_0 \kappa_1 A \sin(u)}{\gamma} \exp\left\{-\gamma\left(x - \dfrac{d}{2}\right)\right\} & x > d/2, \\ \mp\dfrac{k_2 A}{\delta} \cos(\delta x) & -d/2 \le x \le d/2, \\ +\dfrac{k_0 \kappa_1 A \sin(u)}{\gamma} \exp\left\{\gamma\left(x + \dfrac{d}{2}\right)\right\} & x < -d/2. \end{cases} \tag{4.12}$$

and

$$E_z(x) = \begin{cases} A\sin(u) exp\{-\gamma(x - d/2)\} & x > d/2, \\ A \sin(\delta x) & -d/2 \le x \le d/2, \\ A\sin(u) \exp\{\gamma(x + d/2)\} & x < -d/2. \end{cases} \tag{4.13}$$

for RCP (upper sign) and LCP (lower sign) odd modes, respectively where A is an arbitrary constant, which can be determined by total power.
The magnetic fields in the core and the cladding are

$$H_{x,y,z} = \pm \frac{j}{\eta_2} E_{x,y,z} \tag{4.14}$$

for RCP (upper sign) and LCP (lower sign) odd modes.

We can express the enery flow along the z-axis as

$$S_z(x) = \begin{cases} \pm \dfrac{\beta k_0 \kappa_1 A^2 \sin^2(u)}{\eta_2 \gamma^2} exp\left\{-2\gamma\left(x - \dfrac{d}{2}\right)\right\} & \mathrm{x} > d/2, \\ \dfrac{\beta k_2 A^2}{\eta_2 \delta^2} \cos^2(\delta x) & -\mathrm{d}/2 \le \mathrm{x} \le \mathrm{d}/2, \\ \pm \dfrac{\beta k_0 \kappa_1 A^2 \sin^2(u)}{\eta_2 \gamma^2} \exp\left\{2\gamma\left(x + \dfrac{d}{2}\right)\right\} & \mathrm{x} < -d/2. \end{cases} \tag{4.15}$$

for RCP (upper sign) and LCP (lower sign) odd modes.
It is obvious from Eq. (4.15) that S_z is positive for RCP odd modes and negative for LCP odd modes in the cladding, and positive for both RCP and LCP odd modes in the core. On the other hand, we use LHM core which make the energy flux negative in the core for both RCP and LCP odd modes.

4.2.2 Even modes

We again assume a LHM in the core of negative index n_2, so the dispersion relation given in Eq. (4.2) can be divided into two equations as

$$(k_2^2 - \beta^2)^{\frac{1}{2}} \frac{d}{2} = -tan^{-1}\{\frac{k_0 \kappa_1}{k_2}(\frac{k_2^2 - \beta^2}{\beta^2 - k_0^2 \kappa_1^2})^{\frac{1}{2}}\} + m\pi, \qquad m = 0, 1, 2, \ldots \tag{4.16}$$

for RCP even modes, and

$$(k_2^2-\beta^2)^{\frac{1}{2}}\frac{d}{2}=tan^{-1}\{\frac{k_0\kappa_1}{k_2}(\frac{k_2^2-\beta^2}{\beta^2-k_0^2\kappa_1^2})^{\frac{1}{2}}\}+m\pi, m=1,2,3,\ldots \quad (4.17)$$

for LCP even modes.

We can obtain the normalized cutoff frequencies (V) by setting $\beta \to k_0\kappa_1$ in the dispersion Equations (4.16) and (4.17)

$$V=k_0d=\frac{(2m+1)\pi}{(n_2^2-\kappa_1^2\ )^{1/2}}, m=0,1,2,\ldots \quad (4.18)$$

for RCP even modes, and

$$V=k_0d=\frac{(2m-1)\pi}{(n_2^2-\kappa_1^2\ )^{1/2}}, m=1,2,3,\ldots \quad (4.19)$$

for LCP even modes.

We can express the electromagnetic fields in explicit forms as

$$E_x(x)=\begin{cases}-\dfrac{j\beta A\cos(u)}{\gamma}exp\left\{-\gamma\left(x-\dfrac{d}{2}\right)\right\} & \mathrm{x}>d/2,\\ +\dfrac{j\beta A}{\delta}\sin(\delta x) & -\mathrm{d}/2\le \mathrm{x}\le \mathrm{d}/2,\\ +\dfrac{j\beta A\cos(u)}{\gamma}\exp\left\{\gamma\left(x+\dfrac{d}{2}\right)\right\} & \mathrm{x}<-d/2.\end{cases} \quad (4.20)$$

$$E_y(x)=\begin{cases}-\dfrac{k_0\kappa_1 A\cos(u)}{\gamma}exp\left\{-\gamma\left(x-\dfrac{d}{2}\right)\right\} & \mathrm{x}>d/2,\\ \pm\dfrac{k_2 A}{\delta}\sin(\delta x) & -\mathrm{d}/2\le \mathrm{x}\le \mathrm{d}/2,\\ +\dfrac{k_0\kappa_1 A\cos(u)}{\gamma}\exp\left\{\gamma\left(x+\dfrac{d}{2}\right)\right\} & \mathrm{x}<-d/2.\end{cases} \quad (4.21)$$

and

$$E_z(x) = \begin{cases} A\cos(u)exp\left\{-\gamma\left(x-\frac{d}{2}\right)\right\} & \mathrm{x} > d/2, \\ \mathrm{A}\cos(\delta x) & -\mathrm{d}/2 \le \mathrm{x} \le \mathrm{d}/2, \\ A\cos(u)\exp\left\{\gamma\left(x+\frac{d}{2}\right)\right\} & \mathrm{x} < -d/2. \end{cases} \quad (4.22)$$

for RCP (upper sign) and LCP (lower sign) even modes.

The magnetic fields in the core and the cladding are given by Eq.(4.14). We can express the enery flow along the z-axis in the waveguide as

$$S_z(x) = \begin{cases} \pm\frac{\beta k_0 \kappa_1 A^2\cos^2(u)}{\eta_2 \gamma^2} exp\left\{-2\gamma\left(x-\frac{d}{2}\right)\right\} & \mathrm{x} > d/2, \\ \frac{\beta k_2 A^2}{\eta_2 \delta^2}\sin^2(\delta x) & -\mathrm{d}/2 \le \mathrm{x} \le \mathrm{d}/2, \\ \pm\frac{\beta k_0 \kappa_1 A^2\cos^2(u)}{\eta_2 \gamma^2}\exp\left\{2\gamma\left(x+\frac{d}{2}\right)\right\} & \mathrm{x} < -d/2. \end{cases} \quad (4.23)$$

for RCP (upper sign) and LCP (lower sign) even modes, respectively. It is obvious from Eq.(4.23) that S_z is positive for RCP even modes and negative for LCP even modes in the cladding, and positive for both RCP and LCP even modes in the core. On the other hand, we use LHM core which make the energy flux negative in the core for both RCP and LCP even modes.

4.3 Results and discusion

We can calculate the propagation constants numerically from the dispersion relations (4.7), (4.8), (4.16), and (4.17), then the electromagnetic fields and the energy flow distribution can be calculated.In this section, we use numerical values for the parameters in the core and cladding as

$\mu_1 = \varepsilon_1 = 0, \kappa_1 = 0.1, \mu_2 = (-5 + .001\mathrm{I}) \times \mu_0, \varepsilon_2 = (-5 + .001\mathrm{I}) \times \varepsilon_0,\ \kappa_2 = 0.$

4.3.1 Dispersion curves

Figure (4.2) shows the dispersion curves of odd and even guided modes in the slab chiral nihility cladding and LHM core waveguide for low-order modes. Dashed and solid curves correspond to the odd and even modes, respectively. For LCP odd and even modes, the curves of effective refractive index versus normalized frequency increase rapidly, and the normalized cutoff frequencies (points C_1, C_2 when $n_{eff} = 1$) satisfy Equations(4.10) or (4.19). However, for RCP odd and even modes, the cutoff frequencies where$n_{eff} = 1$ are not the minimum frequencies that waves can propagate so the dispersion curves are bent. For RCP even mode when$m = 0$, there is one solution below cutoff frequency (pointC_1) in some frequency region. For both RCP even and odd modes when$m = 1$, there are two solutions below cutoff frequencies (points C_2, C_3) in some frequency region. Thus the real "cutoff" frequencies correspond to the minimum frequencies (critical points*B* and *D*) that guided wave can propagate. As the normalized frequency increases from the critical points*B* and *D*, dispersion curves bifurcate two branches, which the effective refractive index increases for upper branch and decreases to $n_{eff} = 1$ for lower branch.

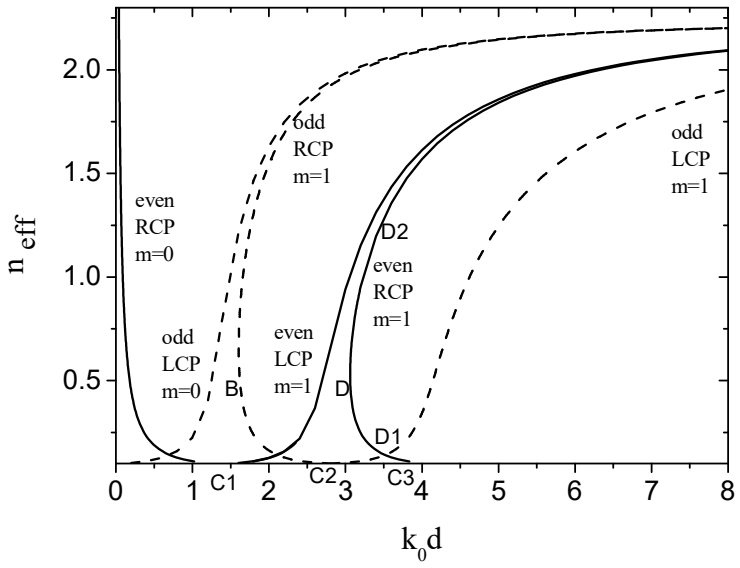

Figure(4.2): Dispersion curves of guided modes in the chiral nihility cladding and negative- indexmaterial core waveguide.

4.3.2 Odd guided modes

Figures (4.3) and (4.4) show the amplitudes of electromagnetic field components and energy flux distribution at normalized frequency $k_0 d = 2.2$ for RCP odd mode when m=1. E_z, H_z are odd functions of x (sin form) and E_x, E_y, H_x, H_y (cos form) are even functions of x. S_z is positive in the cladding and is negative in the core due to the LHM core material. However, there are two propagation constants at $k_0 d = 2.2$.

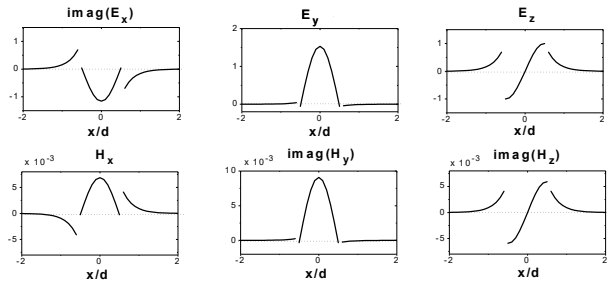

Figure(4.3): Amplitudes of electromagnetic field components at $k_0 d = 2.2$ for RCP odd mode when m=1 ,$n_{eff} = 1.6921$.

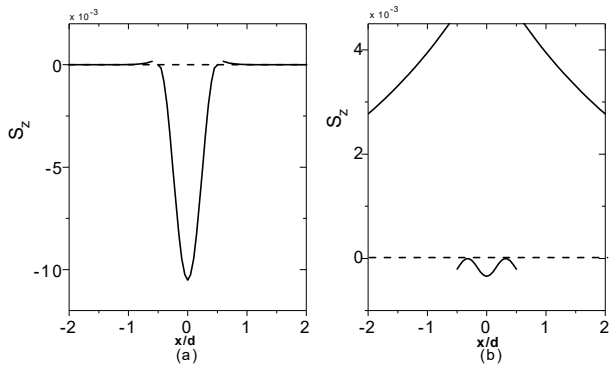

Figure(4.4): Energy flux at $k_0 d = 2.2$ for RCP odd mode when m=1, (a)$n_{eff} = 1.6921$; (b) $n_{eff} = 0.1284$.

Figures (4.5) and (4.6) show the amplitudes of electromagnetic field components and energy flux distribution at normalized frequency $k_0 d = 2$ for LCP odd mode when m=0. E_z, H_z are odd functions of x (sin form) and E_x, E_y, H_x, H_y (cos form) are even functions of x. S_z is negative in both the core and the cladding due to the negative refractive index of the core.

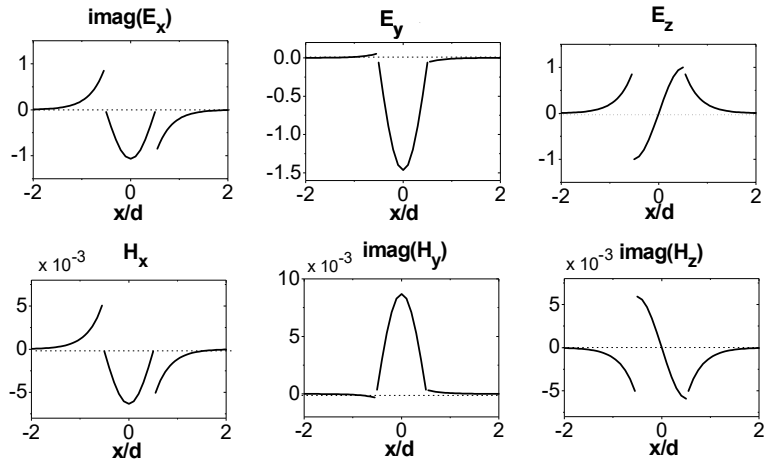

Figure(4.5): Amplitudes of electromagnetic field components at $k_0 d = 2$ for LCP odd mode when m=0.

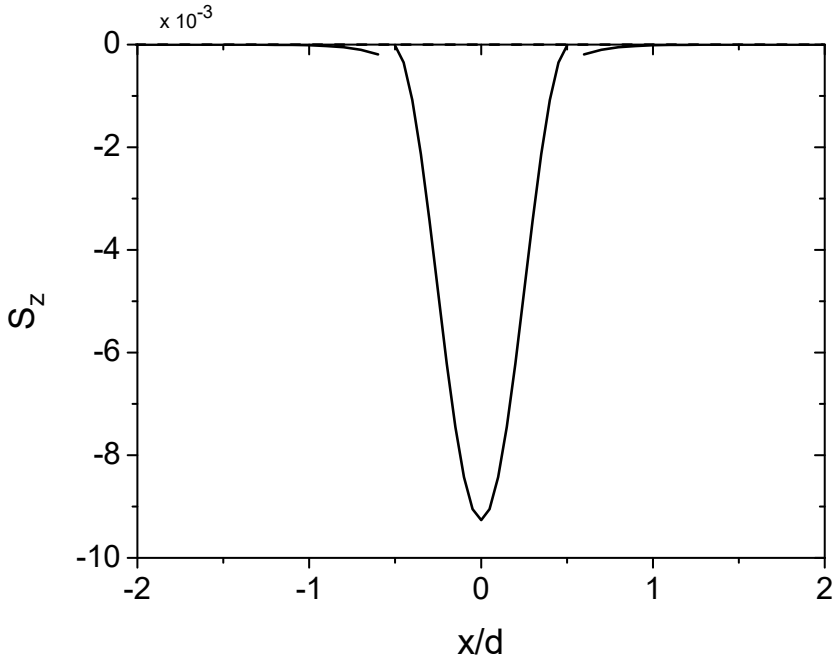

Figure(4.6): Energy flux at $k_0 d = 2$ for LCP odd mode when m=0.

4.3.3 Even guided modes

Figures (4.7) and (4.8) show the amplitudes of electromagnetic field components and energy flux distribution at normalized frequency $k_0 d = 0.5$ for RCP even mode when m=0. E_z, H_z are even functions of x (cos form) and E_x, E_y, H_x, H_y are odd functions of x (sin form). S_z is positive in the cladding and is negative in the core as expected.

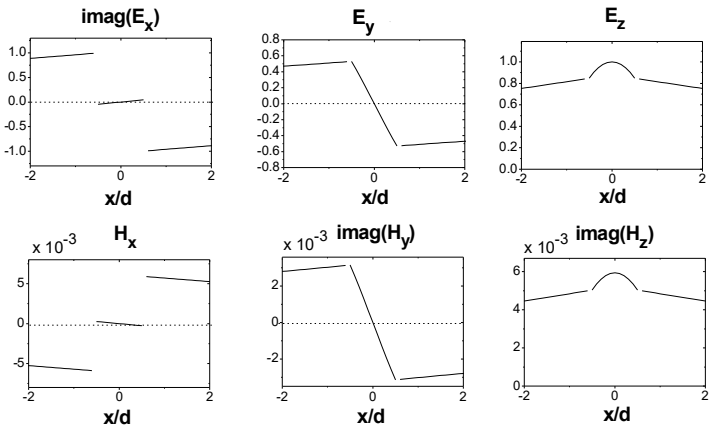

Figure(4.7): Amplitudes of electromagnetic field components at $k_0 d = 0.5$ for RCP even mode when m=0.

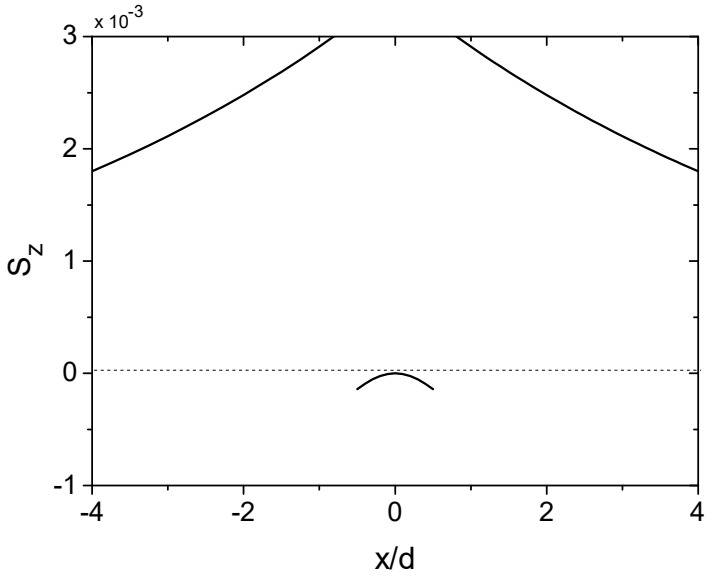

Figure(4.8): Energy flux at $k_0 d = 0.5$ for RCP even mode when m=0.

Figures (4.9) and (4.10) show the amplitudes of electromagnetic field components and energy flux distribution at normalized frequency $k_0 d = 3$ for LCP even mode when m=1. E_z, H_z are even functions of x (cos form) and E_x, E_y, H_x, H_y (sin form) are odd functions of x. S_z is negative in both the core and the claddings.

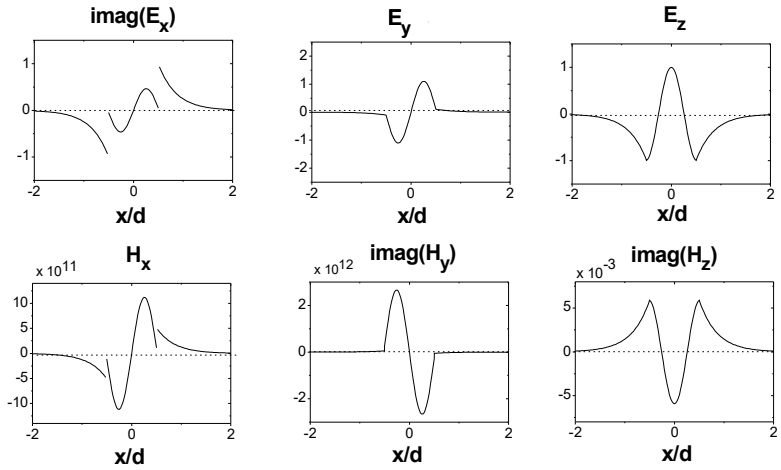

Figure(4.9): Amplitudes of electromagnetic field components at $k_0 d = 3$ for LCP even mode when m=1.

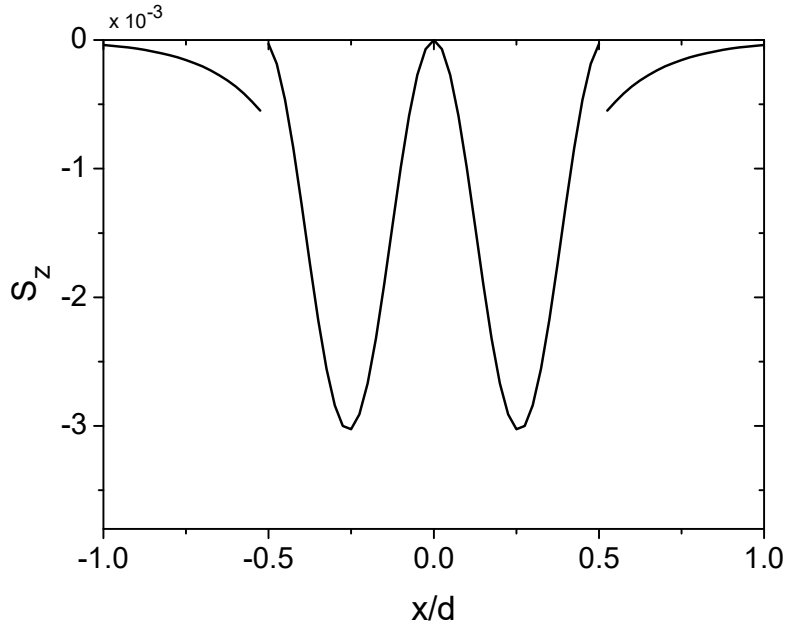

Figure(4.10): Energy flux at $k_0 d = 3$ for LCP even mode when m=1.

The results of this thesis work are consistent with whose in (Dong, 2009) eventhough Dong's work treats a waveguide structures comprising chiral nihility core or claddings with right-handed materials. We analytically present the dispersion relations and the characteristices of the propagation of electromagnetic waves in a waveguide structures consist of chiral nihility core or claddings with left-handed material which make the derivation of the dispersion relations become more difficult.

Conclusions

The dispersion equations of three-layered asymmetric and symmetric chiral slab waveguides in which both the core and claddings are chiral materials were derived. Chiral nihilityproperity where the permitivity ε and permeability μ tend to be zero was considered. In this work, Two special structures of chirowaveguides were presented. The first one consists of a chiral nihility core and LHMs claddings. The other is chiral nihility claddings and LHMs core waveguides. The dispersion equations for odd and even guided modescan be divided into two equations which correspond toright-handed circulary polarized lightRCP and left- handed circulary polarized ligh LCP modes. For each waveguide structure we study odd and even guided modes. For odd and even guided modes,the dispersion equations, normalized cutoff frequencies, electromagnetic fields, and energy flow of RCP and LCP modes were derived in explicit forms. A numerical results for typical chirality parameters of several guided modes were given and plotted. Some novel features such as abnormal dispersion curves in the chiral nihility waveguides were mentioned.For LCP odd and even modes, the curves of effective refractive index versus normalized frequency increase monotonically.However, for RCP odd and even modes, dispersion curves are no longer increasing monotonically, but are bent, and the cutoff frequencies where $n_{eff} = 1$ are not the minimum frequencies that waves can propagate. Thus the cutoff frequencies here are not really "cutoff". The real "cutoff" frequencies correspond to the minimum frequencies that guided wave can propagate.

This analytical work can be benefit in the manufacturing of new waveguides used as antinnas, sensors ,couplers and even solar cells.

References

Abadla, M. A. &Taya, S. A. (2011). Characteristics of left-handed multilayer slab waveguide structure. *The Islamic University Journal (Series of Natural Studies and Engineering), 19*(1),pp. 57-70.

Abraham, M.,&Becker, R. (1960). *The Classical Theory of Electricity and Magnetism*. (2nd ed.). USA: Blackie & Sons Ltd.

Barba, I., Cabeceira, A.C.L., García-Collado, A. J., Molina-Cuberos, G.J., Margineda, J., &Represa, J. (2011). Quasi-planar Chiral Materials for Microwave Frequencies. In Kishk, A. *Electromagnetic Waves Propagation in Complex Matter* ,(pp. 97-116),InTech.

Bassiri, S. (1987). *Electromagnetic wave propagation and radiation in chiral media.*(Unpublished PhD Thesis). California Institute of Technology,Pasadena (California).

Caloz, C., Chang, C., & Itoh, T. (2001, December). Full-wave verification of the fundamental properties of left-handed materials in waveguide configurations. *Journal Of Applied Physics*, *90* (11), pp. 5483-5486.

Chen, H., Wu, B.-I., & Kong, J. A. (2006). Review of electromagnetic theory in left-handed materials. *J. of Electromagn.Waves and Appl*, *20*(15), pp.2137-2151.

Chen, H., Wu,B.-I., Ran, L., Grzegorczyk, T. M., & Kong, J. A.(2006). Controllable left-handed metamaterial and its application to a steerable antenna. *Appl. Phys. Lett.89*, p.053509.

Dong, J. F., & Li, J. (2012, January). Characteristics of guided modes in uniaxial chiral circular waveguides. *Progress In Electromagnetics Research*, *124*, pp. 331-345.

Dong, J., &Xu, C. (2009). Characteristics of guided modes in planar chiral nihility meta-material waveguides. *Progress In Electromagnetic Research B*, *14*, pp. 107–126.

Elsherbeni, A., Demir, V., Al Sharkawy, M., Arvas, E. & Mahmoud, S. (2004). *Electromagnetic Scattering From Chiral Media*. Paper presented at Progress in Electromagnetic Research Symposium, Pisa, Italy.

Ergin, T., Stenger, N., Brenner, P., Pendry, J. B., & Wegener, M. (2010, April). Three-dimensional invisibility cloak at optical wavelengths. *Science, J.328*(5976), pp. 337-339.

Gangwar, K., Paras, &Gangwar, R.P.S. (2014). Metamaterials: Characteristics, Process and Applications. *Advance in Electronic and Electric Engineering*. *4*(1), pp. 97-106.

Griffiths D.J. (1999).*Introduction to electrodynamics*. (3rd edition). USA: prentice hall inc.

Grigorenko, N., Geim, A. K., Gleeson, H. F., Zhang, Y., Firsov, A. A., Khrushchev, I. Y., & Petrovic, J. (2005). Nanofabricated media with negative permeability at visible frequencies. *Nature,438* (7066), pp.335–338.

Kapany, N. S.,&Burke, J. J. (1972). *Optical Waveyuides*. New York: Academic Press.

Kim, Y. (2006).*Novelorganic polymeric and molecular thin-film devices for PhotonicApplications*. (Unpublished PhD Thesis). The University of Maryland (USA).

Koschny, T., Moussa, R., &Soukoulis, C. (2006, March). Limits on the amplification of evanescent waves of left-handed materials.*J. Opt. Soc. Am. B*. *23*(3),pp. 485-489.

Li, L. W., Li, Y. N., Yeo, T. S., Mosig, J.R., & Martin, O.J. (2010, October). A broadband and high-gain metamaterialmicrostrip antenna. *Appl. Phys*. *96*, pp.164-165.

Markoš, P., &Soukoulis, C. M. (2008). *Wave Propagation From Electrons to Photonic Crystals and Left-Handed Materials*. USA: Princeton University Press.

Oksanen, M., Kolivisto, P. K., &lindell, I. V. (1991, August). Dispersion curves and fields for a chiral slab waveguide. *IEEE Proceeding-H*, *138*(4), pp.327-344.

Pelet, P., & Engheta, N. (1990, January). The theory of chirowaveguides. *IEEE Trans. On Antennas and Propagation.38*(1), pp.90-98.

Pendry, J. B. (2000, October). Negative refraction makes a perfect lens. *Phys. Rev.85*(18), pp.3966–3969.

Pendry, J. B., Holden, A. J., Robbins, D. J., & Stewart, W. J. (1998, June). Low frequency plasmons in thin-wire structures. *Phys. Condens. Matter*. *10*(22), pp. 4785-4809.

Pendry, J. B., Holden, A. J., Robbins, D. J., & Stewart, W. J. (1999, November). Magnetism from conductors and enhanced nonlinear phenomena. *IEEE Tran. on Micr. Theo. and Tech*. *47*(11), pp. 2075-2084.

Qiu, C-W.,Burokur, N., Zouhd, S.,& Li, L.-W. (2008,January). Chiral nihility effects on energy flow in chiral materials. *J. Opt. Soc. Am. A*, *25*(1), pp. 55-63.

Sarid, D. &Challener, W. (2010). *Modern Introduction to Surface Plasmons Theory, Mathematica Modeling, and Applications*. USA:Cambridge University Press.

Schuster, A. (1904). *An Introduction to the Theory of Optics*. London: Edward Arnold.

Shadrivov, V. I. (2004, September). Nonlinear guided waves and symmetry breaking in left-handed waveguides.*Photonics and Nanostructures – Fundamentals and Applications 2.* pp.175–180.

Shelby, R. A., Smith, D. R., & Schultz, S. (2001, April). Experimental verification of a negative index of refraction. *Science.292*, pp.77-79.

Smith, D. R. & Kroll, N. (2000, October). Negative Refractive Index in Left-Handed Materials. *Physical Review Letters*, *85*(14), pp.2933-2936.

Sui, Q., Li, C., Li, L. L., & Li, F. (2005). Experimental study of lambda/4 monopole antennas in aleft-handed meta-material.*Progress In Electromagnetics Research.51*, pp. 281–293.

Taya, S. A. (2015). Dispersion properties of lossy, dispersive, and anisotropic left-handed material slab waveguide. *Optik - Int. J. Light Electron Opt.126*(14), pp.1319–1323.

Taya, S. A., &Elwasife, K.Y. (2012, October). Guided modes in a metal-clad waveguide comprising a left-handed material as a guiding layer. *International Journal of Research and Reviews in Applied Sciences (IJRRAS). 13*(1), pp.294-305.

Taya, S. A., &Elwasife, K.Y. (2014).Field profile of asymmetric slab waveguide structure with LHM layers. *J. Nano- Electron. Phys.,6*(2),pp. 02007-02012.

Tellegen, B. D. H. (1948, April). The gyrator, a new electric network element. *Philips Res. Rep*. *3*, pp. 81–101.

Thide, B. (2004). *Electromagnetic Field Theory*. Sweden: Upsilon books.

Veselago,V.G.(1968, Jan-Feb). The electrodynamics of substances with simultaneously negative values of ε and μ. *Sov. Phy.Usp. 10*(4), pp. 509-514.

Wang, Z. J.,& Dong, J. F. (2006). Analysis of guided modes in asymmetric left-handed slab waveguides. *Progress In Electromagnetics Research. 62*, pp.203-215.

Wang, Z.,& Li, S. (2008, June). Quasi-optics of the surface guided modes in a left-handed material slab waveguide.*J. opt. Soc. Am. B. 25*(6), pp. 903-908

.

Wu, B. I., Wang, W., Pacheco, J., Chen, X., Grzegorczyk , T. M., & Kong, J. A. (2005). A study of using metamaterials as antenna substrate to enhance gain. *Progress In Electromagnetics Research*, *51,* pp.295-328.

Xiao, J., Zhang, K., & Gong, L. (1997). Field analysis of a general chiral planer waveguide. *International Journal of lnfrared and Millimeter Waves*, *18*(4), pp.939-948.

Yokota, M., & Yamanaka, Y. (2006, August). Dispersion relation and field distribution for a chiral slab waveguide. International *Journal Of Microwave And Optical Technology, 1*(2), pp. 623-627.

Zhang,C. & Cui, T. J. (2007, November). Negative reflections of electromagnetic waves in chiral media. *Applied Physics Letters*, *91*(19),p.194101.

Zhang, Zh., Wang, Zh., & Wang, L. (2009, October). Design principle of single- or double-layer wave-absorbers containing left-handed materials. *Materials and Design*. *30,* pp. 3908-3912.

Zhang,K., &Li, D. (2008). *Electromagnetic Theory for Microwaves and Optoelectronics*. (2nd ed.). New York: Springer-Verlag Berlin Heidelberg.